



# Climate change remarks in a glacial catchment within Southern Rhaetian Alps: the Fumo Valley case study (Adamello Group, Northern Italy)

Manuel La Licata<sup>1</sup>

<sup>1</sup> Department of Earth and Environmental Sciences, University of Pavia, Via Ferrata 1, 27100 - Pavia, Italy.

MLL, [0000-0001-9106-6408](https://orcid.org/0000-0001-9106-6408).

Rend. Online Soc. Geol. It., Vol. 60 (2023), pp. 51-71, 9 figs., 5 tab., <https://doi.org/10.3301/ROL.2023.32>

## Article

Corresponding author e-mail: [manuel.lalicata01@universitadipavia.it](mailto:manuel.lalicata01@universitadipavia.it)

*Citation:* La Licata M. (2023) - Climate change remarks in a glacial catchment within Southern Rhaetian Alps: the Fumo Valley case study (Adamello Group, Northern Italy). Rend. Online Soc. Geol. It., 60, 51-71, <https://doi.org/10.3301/ROL.2023.32>.

*Guest Editor:* Alessandro Petrocchia

*Submitted:* 24 November 2022

*Accepted:* 28 February 2023

*Published online:* 20 April 2023

*Copyright:* © The Authors, 2023



**SOCIETÀ GEOLOGICA ITALIANA**

FONDATA NEL 1881 - ENTE MORALE R. D. 17 OTTOBRE 1885

## ABSTRACT

In this study, glacier retreat from the end of the Little Ice Age to present time and climatic variations on recent time scale were assessed in the Fumo Valley, which is a small glacial catchment located in the Adamello Group (Southern Rhaetian Alps, Italy). The study area has a high scientific and cultural value as part of the UNESCO Adamello-Brenta Geopark and provides several ecosystem and socio-economic services. Therefore, the assessment of climate change impacts at local scale is essential for a sustainable watershed management, as well as for conservation strategies.

A present-state glacier inventory was elaborated by means of remote sensing using Sentinel-2 satellite images. Then, it was compared to previous published glacier inventories in order to assess numerical and geometric surface variations. Also, two temperature data series related to different thirty-year periods (i.e., 1971-2000 and 1991-2020) were analysed to assess air temperature variations. The results highlight a total surface loss of 5.99 km<sup>2</sup> (-70.9%) between 1850 and 1958. Between 1958 and 2022 a total area reduction of 0.87 km<sup>2</sup> (-35.5%) was observed, which is comparable to other studies carried out at national scale. However, a minor progression phase was observed between 1958 and 1981 (+76.3%), which is partially attributable to the glacial advance episode that occurred between the 1970s and 1980s in the Italian Alps. After, total glacier area declined by 63.4% (1981-2022), with an accelerated regression between 2015 and 2022 (i.e., higher annual rate of variation, formation of ice-contact lakes, tongue separation, and severe glacier fragmentation). The mean annual air temperature rose of 0.6°C, with a greater variation in mean annual maximum temperature (+1°C) than minimum temperature (+0.1°C), and an average temperature increase higher in spring and summer than in autumn and winter.

These results can be interpreted as truthful indicators of climate change impacts occurring at local scale, highlighting the vulnerability of the study area with respect to the predicted future climatic scenarios.

**KEY-WORDS:** Glacier variation, Glacier inventory, Climate Change, Remote sensing, Adamello Group.

## INTRODUCTION

Alpine environments are among the most vulnerable areas with respect to climate change (Hock et al., 2019; IPCC, 2021) due to their peculiar geographic and morphological features, as well as their key role in controlling several ecosystem services. Since the late 19<sup>th</sup> century, the Alpine region has experienced an increase in the annual mean temperature of about 2°C, more than twice the average in the northern hemisphere, with a significant summer warming since 1970 (Auer et al., 2007; Brugnarà et al., 2012). The most accurate climatological models predict an intensification of the already observed trend in the next decades (Gobiet et al., 2014; Rubel et al., 2017), with several implications for both biotic and abiotic systems (Beniston, 2003; Cannone et al., 2008; Diolaiuti & Smiraglia, 2010). The main impacts on mountain systems will include glacier melting, altitudinal shift in permafrost distribution, climbing of the snowline, changes in sediment fluxes, habitat loss, and increase of geomorphological hazards (EEA, 2009; Deline et al., 2015; Hock et al., 2019; Morino et al., 2021). Furthermore, hydrological systems are expected to become more sensitive to climate change, leading to variations in the runoff regime of rivers and changes in the availability of water resources (EEA, 2009).

The variation in glacier extent is generally considered the most easily observed and unambiguous indicator of global warming, which

is impacting worldwide and, in particular, the Alpine region (EEA, 2004; Oerlemans, 2005; Citterio et al., 2007). Most mountain glacial masses have been retreating since the end of the Little Ice Age (LIA; Zemp et al., 2006; Zanoner et al., 2017), but more recently glaciers began melting at rates that cannot be explained only by natural climatic variability (Dyurgerov & Meier, 2000). In particular, between 1850 and 1980 glaciers in the European Alps lost approximately one third of their area and one half of their mass. Moreover, since 1980 another 20 to 30% of ice has melted (EEA, 2004). Despite this general retreat, some minor phases of glacial progression were observed (i.e., around 1890, during the 1910s and from the 1970s to the mid-1980s; Salvatore et al., 2015; D'Agata et al., 2018).

As glacier shrinkage is particularly severe upon the Alps, the recent rapid mass loss of Alpine glaciers in response to climate warming has been widely investigated as reported in literature (e.g., Paul et al., 2004a,b; Citterio et al., 2007; Haeberli et al., 2007; Diolaiuti et al., 2011; D'Agata et al., 2014; Paul et al., 2020). The analysis of satellite data revealed a strong acceleration of glacial shrinkage in the Alps since the 1980s, with a mean decadal rate of area reduction seven times higher than during the 1850-1973 period (Paul et al., 2004a; Paul et al., 2007). Therefore, considering the actual velocity rate of glacial surface reduction (Paul et al., 2020; Sommer et al., 2020), and the projections displayed by future climatic scenarios (e.g., Gobiet et al., 2014), in the next decades the Alpine region may undergo an almost complete loss of glacierised areas (Zemp et al., 2006; Haeberli et al., 2007).

Among the possible methods to analyse the ongoing evolution of glacierised areas, the collection and analysis of glacier inventories can be used to investigate mountain glaciation in a changing climate and potential scenarios on the regional Alpine scale (Paul et al., 2004b; Zemp et al., 2006; D'Agata et al., 2014; Smiraglia et al., 2015). The comparison of various glacier inventories related to different temporal ranges, e.g., by comparing parameters typically considered in glacier inventories, such as glacier area, makes it possible to draw a general picture of the changes that have taken place in a particular glacial region over the past decades (Citterio et al., 2007; Maragno et al., 2009).

Over the last decades, Italian glaciers have experienced a strong area reduction which is comparable to other Alpine glacierised sectors in terms of magnitude and rates of reduction (Smiraglia et al., 2015). The comparison between the total glacierised area reported in the Italian Glacier Inventory (IGI) of the early 1960s (CGI-CNR 1959; 1961a; 1961b; 1962) and that in the New Italian Glacier Inventory (NIGI) published in 2015 (Smiraglia & Diolaiuti, 2015) highlights an overall reduction of about 30% (i.e., from 526.88 km<sup>2</sup> in the 1960s to 369.90 km<sup>2</sup> in the present time; Smiraglia et al., 2015). The strongest area reduction is the one affecting small glaciers (that is, glaciers with an area < 1 km<sup>2</sup>), which cover approximately 80% of the census in the Alps, making an important contribution to water resources (Citterio et al., 2007; D'Agata et al., 2018).

On the other hand, in the periglacial environment Alpine permafrost and permafrost related landforms are experiencing significant changes in response to the current climatic warming (Haeberli & Gruber, 2009; Seppi et al., 2019). This fact has potential consequences on their hydrological role in providing

water resources (Jones et al., 2009). Moreover, it may directly or indirectly influence the occurrence of slope instability processes and related geomorphological hazards (Chiarle & Mortara, 2008; Harris et al., 2009; Schoeneicht et al., 2011).

The degradation of the cryosphere (i.e., glaciers, ice, and permafrost) is of particular interest from a socio-economic point of view. In particular, many minor Alpine catchments exploited for hydropower generation would undergo marked changes in their seasonal water discharge in the case of significant deglaciation events (Citterio et al., 2007; Jones et al., 2019). In the Italian Alps, several small artificial basins for hydroelectric power production provide 25% of the total national electric production (Ajassa et al., 1994). The predicted disappearance of small glaciers in the next decades may have critical consequences on the hydrological cycle on a catchment scale (Bocchiola & Diolaiuti, 2010), triggering several socio-economic challenges related to ecosystem services deterioration (Haeberli & Beniston, 1998). Therefore, the impacts of prolonged and accelerated glacier melting on river flow regimes, water resources, and hydropower production capacity will be a key issue for energy production in the next decades (Grossi et al., 2013; Ravazzani et al., 2015; EEA, 2017). For this reason, it is essential to investigate the variation of climatic parameters such as air temperature and changes in the cryosphere within small glacial catchments that provide water resources and socio-economic services (see, e.g., Giaccone et al., 2015; Colombo et al., 2016).

This study is aimed at assessing glacier surface reduction from the end of the LIA to present time and climatic temperature variations on recent time scale in the Fumo Valley. It is a small glacial catchment located in the Adamello Group (Southern Rhaetian Alps, Trentino, Northern Italy). It comprises an artificial basin exploited for hydroelectric power generation with a prevalent feeding provided by water runoff flows driven by the annual melting of glaciers included in its boundaries. Furthermore, the study area is part of the UNESCO Adamello-Brenta Geopark since it includes several protected areas of naturalistic and cultural interest. Thus, it represents an area of great value for both scientific and tourist purposes. Hence, the assessment of climate change impacts at local scale is essential for sustainable watershed and land management, as well as for conservation strategies.

## STUDY AREA

### Geographic setting

The study was carried out in the Fumo Valley (46°9' - 46°2' N; 10°29' - 10°36' E), which is located in the Autonomous Province of Trento (APT; Trentino, Northern Italy; Fig. 1a,b) and belongs to the Adamello Group (Southern Rhaetian Alps). In particular, the study area coincides with the catchment upstream of the Malga Bissina lake (Fig. 1c,d), which is an artificial basin for hydroelectric power generation. The catchment stretches N-S for ~ 12 km with an extent of 51 km<sup>2</sup> and an altitudinal range varying from 1770 to 3463 m a.s.l. (Mt. Caré Alto peak; Fig. 1c,d). It is in the uppermost and northern part of the Chiese hydrographic basin, since the Chiese river originates from the glacier located at the head of the valley (i.e., Vedretta di Fumo; Fig. 1c).

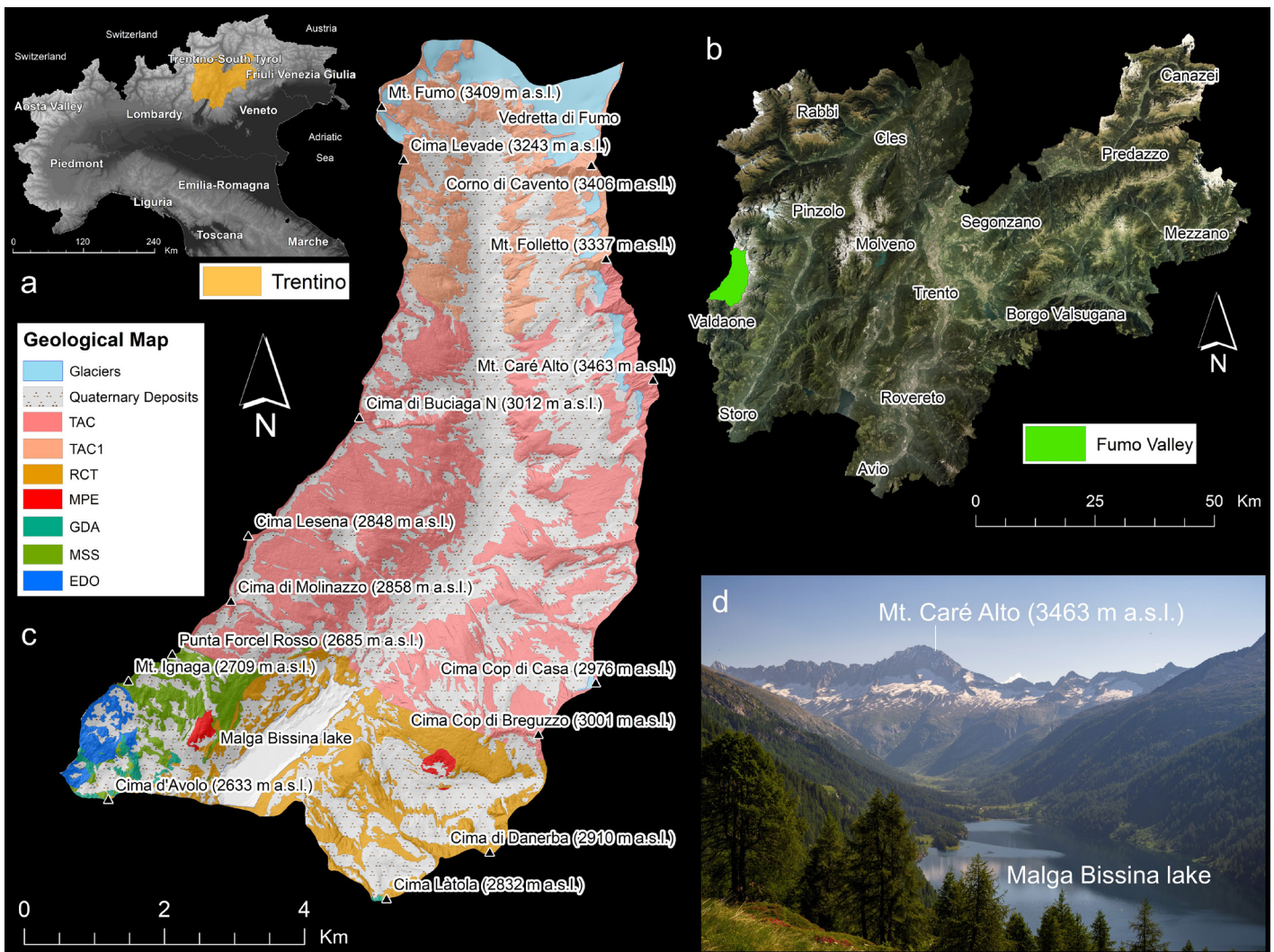


Fig. 1 - (a,b) Geographical setting of the Fumo Valley within the Autonomous Province of Trento (APT; Trentino), Northern Italy. (c) Simplified Geological sketch map of the Fumo Valley (modified after Brack et al., 2008). TAC = Western Adamello Tonalite; TAC1 = Central Adamello Tonalite; RCT = Re di Castello Tonalite; MPE = Malga Persec Trondhjemitic and Leucogranite; GDA = igneous mafic rocks; MSS = Mt. Ignaga-Forcel Rosso succession (all the units included in the succession are grouped together); EDO = Edolo Schists. Glaciers and Quaternary Deposits are also represented. Shapefile data are provided by the Geological Survey, Civil Protection Department, APT (CARG Project; <http://www.protezionecivile.tn.it/territorio/Cartografia/>). (d) Panoramic view of the study area. WMS data sources: DTM Italia 20m (© Ministero dell'Ambiente e della Tutela del Territorio e del Mare – Geoportale Nazionale; [www.pcn.minambiente.it/](http://www.pcn.minambiente.it/)); Digital Orthophoto 2015 (© APT - Portale Geocartografico Trentino; [www.territorio.provincia.tn.it/](http://www.territorio.provincia.tn.it/)).

The area is fully included within the UNESCO Adamello-Brenta Geopark since it comprises several protected areas of naturalistic and geological interest. In addition, the study area is part of the Natura 2000 Network, including the SPA IT3120158 “Adamello-Presanella” and the SACs IT3120175 “Adamello” and IT3120166 “Re di Castello-Breguzzo”.

### Structural and geological setting

The Fumo Valley is included in the geological-structural context of the large Adamello batholith of Eocene to Oligocene age (Callegari, 1985; Callegari & Brack, 2002), which was emplaced at shallow levels into the Southalpine pre-Permian crystalline basement and the Permo-Mesozoic sedimentary cover rocks (John & Blundy, 1993). The batholith, which is exposed over an area greater than 670 km<sup>2</sup>, is the largest and oldest intrusive body of the post-collisional Alpine Tertiary magmatism along the Periadriatic fault system (Bianchi et

al., 1970; Dempsey et al., 2014). It is located in a wedge-like crustal sector of the Southern Alps, bounded by the Tonale Line to the north and the Giudicarie Line to the east (“Periadriatic Igneous Province”; Callegari & Dal Piaz, 1973).

According to Callegari & Brack (2002) and Brack et al. (2008), in the upper and central sectors the Fumo Valley belongs to the Adamello pluton, which includes the Western (TAC) and Central (TAC1) Adamello Tonalite units of Upper Eocene age (Fig. 1c). Otherwise, the lower sector is part of the Re di Castello pluton, which includes the Malga Persec Trondhjemitic and Leucogranite unit (MPE; Middle-Upper Eocene), and Re di Castello Tonalite unit (RCT; Middle Eocene) (Fig. 1c). The main lithologies are massive coarse-grained hornblende biotite tonalite (TAC), massive medium to coarse-grained leucocratic tonalite (TAC1), garnet-bearing biotite leucogranite and two-mica trondhjemitic (MPE), and relatively fine-grained leucocratic to mesocratic biotite-hornblende tonalite (RCT). In the SW sector, igneous mafic rocks (GDA; e.g., hornblende

gabbro and biotite-bearing hornblende gabbro) of Eocene age are also present (Fig. 1c; [Callegari & Brack, 2002](#); [Brack et al., 2008](#)).

The metamorphic basement (pre-Permian) and the volcanic, clastic, and carbonate sedimentary cover rocks (Permian-Triassic) of the Southern Alpine continental crust outcrop limitedly to the SW margin of the study area ([Brack et al., 2008](#)). They are in contact with TAC at north-east and RCT, MPE, and GDA at south-east (Fig. 1c). Hence, both of them were thermally overprinted by the metamorphic aureole produced by the Tertiary Adamello intrusions near the contact zones ([Callegari & Brack, 2002](#)). The basement is represented by the Edolo Schists (EDO; Fig. 1c; “paraschists complex”, Lombardy sector), which are characterised by a Variscan low-medium grade metamorphic imprint and a regional schistosity in condition of greenschist facies. At regional scale, EDO includes chlorite-sericite-quartz phyllites, albitic micaschists, and two-mica albitic paragneisses. Instead, the thermal overprints are purple cornubianites with biotite, garnet, andalusite and sillimanite ([Brack et al., 2008](#)).

The study area includes one of the most complete and well-preserved metasedimentary successions at the regional scale (i.e., Mt. Ignaga-Forcel Rosso sedimentary succession; MSS; Fig. 1c; [Brack et al., 2008](#)). It starts from the Val Savio Basal Volcanics (Lower Permian) as oldest unit to the Breno Formation (Lower-Middle Carnian) as younger one. In the study area, these metamorphosed cover rocks are mostly represented by massive cornubianites and marbles with several neof ormation minerals, showing evidence of subsequent Alpine deformative phases ([Brack et al., 2008](#)).

Quaternary deposits related to glacial, periglacial, fluvial, and slope processes are widespread in the study area (Fig. 1c; see also next Section).

Several faults and master joints can be identified in the study area, whose development is related to the Gole Larghe-Val di Genova Line system. Some authors pointed out a link between these structural elements and sin- and post-intrusive deformative phases which affected the area until recent times ([Callegari, 1983](#)).

## Geomorphological setting

The geomorphological landscape of the Fumo Valley is the result of both litho-structural features and glacial modelling particularly during Local Last Glacial Maximum (LLGM), Lateglacial, and LIA ([Orombelli et al., 2005](#); [Orombelli, 2011](#)).

The control by extensive regional fault systems is reflected by the structural-morphological pattern of the valley, as well as the configuration of the hydrographic network. The latter shows a centrifugal arrangement diverging radially from the top areas of the massif (as for other secondary valleys, e.g., Adamè, Salarno, Miller, Baitone, and Avio valleys; [Carton & Baroni, 2017](#)).

The Fumo Valley is a typical U-shaped trough glacial valley (Fig. 1d) within the Adamello-Brenta Geopark. The evidence of its glacial modelling is well preserved thanks to the lithological and geomechanical characteristics of tonalitic rocks ([Brack et al., 2008](#)), which make them less susceptible to frost shattering. Slopes are characterised by steep slopes interrupted by well-developed glacial shoulders. Other glacial landforms such as small hanging valleys, cirques, *roches moutonnées*, *arêtes* and different successions of glacial basins and steps can be widely observed

([Baroni et al., 2014](#)). Lateglacial till deposits are widespread in the study area. They are generally stabilised by the vegetation cover and well-developed soils (e.g., *Enti-Umbric*, *Umbri-Densic* and *Skeletal Podzols*, and *Humic Umbrisols*; [Sartori et al., 2005](#); IUSS Working Group WRB). Several LIA moraines can be observed in the proximity of existing or only recently extinct glaciers, especially in the northern and eastern sectors of the study area. In some cases, they show the evidence of the paraglacial stage of development ([Slaymaker, 2011](#); i.e., gullying on their flanks; [Mercier et al., 2009](#)).

In the study area, there are also several rock glaciers ([Baroni et al., 2004](#)). Most of them can be classified as “intact” landforms, while few are “relict” ones ([Seppi et al., 2012](#)). The current geomorphic processes are mainly related to the periglacial morphoclimatic readjustment, such as mass movements due to slope instability and selective slope degradation processes, cryonival, and glacio-fluvial processes ([Baroni & Carton, 1990b](#)). At the toe of valley slopes, debris production, mass movements, debris flows, running water, and snow avalanches often generate composite debris cones ([Gentili et al., 2020](#)).

From the glaciological standpoint, the catchment includes several glaciers and glacierets ([Smiraglia & Diolaiuti, 2015](#)) (Fig. 1c). They represent the only remnants of the glacial context in which the territory was modelled during Quaternary ([Carton & Baroni, 2017](#)). Most of them are cirque glaciers. The Vedretta di Fumo is the largest glacier within the study area, as it represents the southern glacial tongue of the Lobbia glacier flowing into the Fumo Valley. The two glaciers are divided by an ice-divide delimiting the Fumo Valley catchment at north ([Baroni & Carton, 1990a](#)). Thus, the drainage system in the study area is characterised by a marked glacial hydrological regime with a minor nival-pluvial feeding.

## Climatic setting

The Fumo Valley is located in the transition zone between southern and inner Alpine areas. The former are characterised by a humid climate with precipitation ranging from 1800 to 2500 mm yr<sup>-1</sup> concentrated in spring and autumn. Instead, inner Alpine areas exhibit a more continental climate with precipitation mostly occurring during winter and ranging from 1000 to 1200 mm yr<sup>-1</sup> ([Baroni et al., 2004](#); [Carton & Baroni, 2017](#)). In particular, the study area is characterised by a humid temperate climate at lower elevations, shifting towards a boreal snowy humid climate at middle-high elevations. At higher altitudes, the climate is polar ([Eccel et al., 2012](#)). The average vertical thermal gradient in the Adamello Group is 0.59°C/100 metres, whereas the mean annual precipitation shows a general increase with altitude ([Baroni et al., 2004](#)). Snowy rainfalls generally occur from October to May, with rare precipitation events in September. At higher altitudes, snow cover remains on the ground until May-June ([Carton & Baroni, 2017](#)).

## MATERIALS AND METHODS

### Assessment of present number and extent of glaciers

The assessment of present number of glaciers as well as the estimation of their extent within the Fumo Valley were based on

the elaboration of a present-state glacier inventory (VGI\_2022) by means of remote sensing using Sentinel-2 (S2) MSI satellite images (Drusch et al., 2012; Paul et al., 2020). A series of different top-of-atmosphere reflectance (TOAR) images starting from 1<sup>st</sup> August 2022 to 30<sup>th</sup> September 2022 was visualised and examined through the Copernicus Open Access Hub (<https://www.scihub.copernicus.eu/>). The selection of TOAR products was aimed at dealing with cloud-free images and the absence of snow cover outside the glacierised surface on slopes (Paul et al., 2007). Hence, two different tiles entirely covering the study area were properly selected and downloaded:

- S2B\_MSIL1C\_20220801T100559\_N0400\_R022\_T32TPS\_20220801T121930, (01/08/2022);
- S2B\_MSIL1C\_20220923T101649\_N0400\_R065\_T32TPS\_20220923T140342, (23/09/2022).

The 01/08/2022 TOAR provided the best quality product for glacier identification and mapping, especially thanks to the almost total absence of clouds and cast shadows under steep cirque scarps, as well as to the deficiency of snow cover. Nevertheless, in spite of the worse quality due to the local presence of cast shadows, the 23/09/2022 TOAR was used for the validation of the main glacier boundaries at the end of the ablation season.

From all tiles, MSI bands 2, 3, 4, 8 and 11 (i.e., Blue, Green, Red, Near-Infrared and Shortwave Infrared; Kääb et al., 2016) were downloaded and managed using the ArcMap 10.3.1 software (© Esri). MSI2, MSI3, MSI4 and MSI8 bands are 10 metres of resolution, whereas MSI11 band is 20 metres of resolution (Drusch et al., 2012).

The identification of the main glacial bodies was based mainly on the high spectral reflectance of snow and glacier ice in the visible and near infrared (VNIR) compared to the high spectral absorption in the shortwave infrared (SWIR) (Dozier, 1989). In particular, snow and ice are bright in the VNIR bands (high reflectance), but very dark (low reflectance) in the SWIR band. Thus, the ratio between a VNIR and a SWIR band gives high values over glacier ice and snow, and very low values over all other terrain, as the latter is often much brighter in the SWIR than in the VNIR (Paul et al., 2020). These differences in spectral reflectance make it simple to distinguish glacierised surfaces from other objects (e.g., rock outcrop, lakes, vegetation, and debris), especially in the case of debris-free glaciers and glacierised surfaces covered by snow. Therefore, two different band ratios were calculated using the ArcMap Image Analysis Tool: MSI4/MSI11 (i.e., Red/SWIR) and MSI8/MSI11 (i.e., NIR/SWIR). In order to calculate the ratios, the SWIR band (MSI11) was resampled from 20 to 10 metres using a simple bilinear interpolation (Paul et al., 2016). Additionally, different multi-band false composite colour (FCC) images were elaborated: MSI8, MSI4, MSI2, i.e., “NIR, Red, Blue”; MSI2, MSI3, MSI4, i.e., “Blue, Green, Red”; MSI11, MSI8, MSI3, i.e., “SWIR, NIR, Green” (Serandrei-Barbero & Zanon, 1993; Paul et al., 2007, 2013). In particular, FCC images permit to better distinguish between glaciers and water bodies in their proximity, as well as the presence of debris above glacier surface thanks to its different colouring due to high humidity if compared to dry debris deposited on slopes (Fea et al., 2013). Hence, the analysis of FCC images

allowed to identify and localise those glacier parts and glacierets which were not well detectable with band ratio techniques (i.e., due to the presence of a partial debris cover and dirty ice), as well as to identify misclassified glaciers such as isolated snow patches on slopes and/or water bodies.

The multi-band images were compared to the band ratios and the natural colour RGB images in order to accomplish an accurate visual interpretation of glacier extent and boundaries. In addition, these images were compared to the high-resolution hillshade relief map derived from the LiDAR DTM 2014 (APT; *Portale Geocartografico Trentino*; <http://www.territorio.provincia.tn.it/>) in order to better delineate glacier boundaries below steep reliefs (e.g., cirque glaciers). Then, glaciers were manually digitised one by one creating a polygon shapefile and their area was extracted using the ArcMap software. For this reason, no thresholds and masks for automated glacier mapping were applied to the band ratios (e.g., see Paul et al., 2007, 2016, 2020).

### Assessment of glacier numerical and geometric variations

The assessment of numerical and geometric variations of the Fumo Valley glaciers was based on the comparison of glacier inventories related to different temporal periods (D'Agata et al., 2014, 2018). In particular, the following published databases were analysed:

- LIA Trentino Glacier Inventory (LGI\_1850) (Zanoner et al., 2017). Data referring to 1850 by convention as maximum LIA glacier extent (Ivy-Ochs, 2009);
- CGI Italian Glacier Inventory (IGI\_1958). Data referring to 1958 (CGI-CNR 1959, 1962);
- World Glacier Inventory (WGI\_1981). Data referring to 1981 (Haeberli et al., 1989; WGMS & NSIDC, 1999; [https://www.nsidc.org/data/glacier\\_inventory/](https://www.nsidc.org/data/glacier_inventory/));
- Trentino Glacier Inventory 2003 (TGI\_2003). Data referring to 2003 (*Portale Geocartografico Trentino*; <http://www.territorio.provincia.tn.it/>);
- Trentino Glacier Inventory 2015 (TGI\_2015). Data referring to 2015 (*Portale Geocartografico Trentino*; <http://www.territorio.provincia.tn.it/>).

At first, the LGI\_1850 database was elaborated as LIA and post-LIA glacial deposits, as part of the APT Glaciers and Little Ice Age Hazard Map, by means of remote sensing and digital mapping using a hillshade relief map derived from a 2 m LiDAR DEM and high-resolution digital orthophotos. Next, the maximum extent of glaciers during LIA was derived on the basis of geomorphological features of glacial deposits, archival information, and previously published studies (Zanoner et al., 2017). The IGI\_1958 database was developed by analysing already existing maps (scale 1:25000, published by the Italian Military Geographic Institute), as well as through field surveys (CGI-CNR 1959, 1962). The WGI\_1981 database was developed primarily by aerial photo analysis (Diolaiuti et al., 2019). The TGI\_2003 and TGI\_2015 databases were elaborated by the APT Prevention and Risk Service, by means of field surveys, photointerpretation, and digital mapping using high

resolution aerial images and laser-scanning surveys carried out in September 2003 and September 2015 respectively.

The total number of active and extinct glaciers, as well as the geometric data of single glaciers, were acquired for each glacier inventory. Data related to IGI\_1958 and WGI\_1981 were extracted from literature (i.e., from CGI-CNR 1959, 1962; Haeberli et al., 1989; Smiraglia & Diolaiuti, 2015), whereas data related to LGI\_1850, TGI\_2003 and TGI\_2015 were extracted by querying the available shapefile databases using the ArcMap software.

The total surface variation, as well as the percentage and annual rates of variation, were calculated for the following temporal ranges: 1850-1958; 1958-1981; 1981-2003; 2003-2015; 2015-2022; 1850-2022; 1958-2022; 1981-2022. In some cases, it was necessary to sum different glacial units in the reference inventory to compare them with previous ones in order to deal with glacier fragmentation.

The size classification proposed by Paul et al. (2004a,b) was adopted to classify glaciers: < 0.1 km<sup>2</sup>, 0.1-0.5 km<sup>2</sup>, 0.5-1 km<sup>2</sup>, 1-2 km<sup>2</sup>, 2-5 km<sup>2</sup>, 5-10 km<sup>2</sup> and > 10km<sup>2</sup>. Also, glaciers were named and classified into “glacier types” according to the NIGI (Smiraglia & Diolaiuti, 2015).

### Assessment of temperature climatic variations

Daily temperature data related to the thirty-year period 1991-2020 were analysed in order to achieve a characterisation of the present climatic conditions. Two different weather stations located at Malga Bissina lake dam and managed by the APT Provincial Meteorological Service (*Meteo trentino*; <https://www.meteotrentino.it/>; Tab. 1) were used: T0156 provided data from 1991 to 2003, while T0373 provided data from 2004 to 2020. The two stations are ~ 200 metres apart with a difference in altitude < 10 metres. Meteorological parameters were calculated according to the definition of the *Annale Idrologico* (i.e., calculated during the 24 hours elapsed from the 9<sup>th</sup> solar hour of the previous day to the 9<sup>th</sup> solar hour of the current day).

Then, 305 synchronous temperature daily data, related to a temporal range in which the two stations worked together between 2002 and 2003, were compared and analysed to assess their correlation coefficient. Subsequently, considering a correlation coefficient equal to 0.96, the temperature data series of the two weather stations were properly merged to obtain a thirty-year period.

Next, monthly temperature indicators (MTIs; i.e., mean temperature, mean minimum and maximum temperatures) were calculated for each year through the National System for the Elaboration of Climatic Data (SCIA) developed by the Italian Institute for Environmental Protection and Research (ISPRA; <https://www.scia.isprambiente.it/>; Desiato et al., 2007, 2011). In particular, SCIA system provides automated processing and validation procedures based on both availability and quality of daily data dealing with inhomogeneities and gaps within the data series (for further details

see Baffo et al., 2005a,b and Fioravanti et al., 2016). Then, the standard monthly, annual and seasonal normals of temperature data related to the 1991-2020 period were calculated using MTIs (WMO, 2015, 2017). In this paper, the following nomenclature for monthly and annual normals is used: mean monthly (MMAT) and annual air temperature (MAAT); mean monthly (MMmT) and annual minimum air temperature (MAMt); mean monthly (MMMT) and annual maximum air temperature (MAMT).

In order to assess climatic variations, the normals related to the 1991-2020 period were compared to those related to the 1971-2000 period (T0156; Tab. 1). The latter were previously calculated from an MTI dataset processed through the SCIA system and published in Desiato et al. (2015).

The average vertical thermal gradient of 0.59°C/100 metres calculated for the Adamello-Presanella Group by Baroni et al. (2004) was applied to the monthly and annual temperature normals for each thirty-year period. Then, the Köppen-Geiger climate classification system (Kottek et al., 2006) was applied to normals calculated every 100 metres to identify and characterise the altitudinal climatic belts (Rubel et al., 2017). Finally, the mean annual isotherms corresponding to a MAAT of 0, -1 and -2°C (Baroni et al., 2004) were calculated for the periods 1971-2000 and 1991-2020.

## RESULTS

### Present state glacier inventory of the Fumo Valley

Multi-band ratios and composite FCC images proved to be useful tools to examine the presence of glacierised surfaces and to delineate glacier boundaries in order to elaborate a present state glacier inventory of the study area (VGI\_2022; Fig. 2; Fig. 3; Tab. 2).

The MSI4/MSI11 and MSI8/MSI11 ratios provided roughly the same results in the characterisation of debris-free glacierised surfaces owing to their spectral properties (Paul et al., 2016, 2020). Fig. 2a highlights the presence of several medium- and small-size glaciers which are represented with a dark blue colouring as pixels with highest ratio values due to the high spectral reflectance in MSI4 and MSI8 bands (Dozier, 1989). Furthermore, some glaciers are locally characterised by lower MSI4/MSI11 ratio values (i.e., light blue and greenish colouring), especially in marginal areas, likely due to the presence of slightly dirty ice (Fig. 2a) (Paul et al., 2013). Otherwise, bare rock surfaces and debris cover on slopes are characterised by medium-low ratio values (yellow colouring), whereas the vegetation has the lowest values (orange and red colouring) (Fig. 2a). The same results were obtained by processing the MSI11,MSI8,MSI3 FCC image, where glacierised areas are represented with blue and petrol green colours, bare rocks and debris on slopes with pink to purple, and vegetation with yellowish colouring (Fig. 2b; Paul et al., 2007, 2013).

**Table 1 - Metadata of the two weather stations located at the Malga Bissina dam (Fumo Valley). \*: only for precipitation measurements.**

Code	Name	Latitude	Longitude	Altitude	Start date	End date
T0156	Diga Malga Bissina	46°03'17.3" N	10°30'50.3" E	1792 m a.s.l.	01-01-1960*	31-10-2005
T0373	Malga Bissina	46°03'10.5" N	10°30'50.8" E	1785 m a.s.l.	03-10-2002	In function

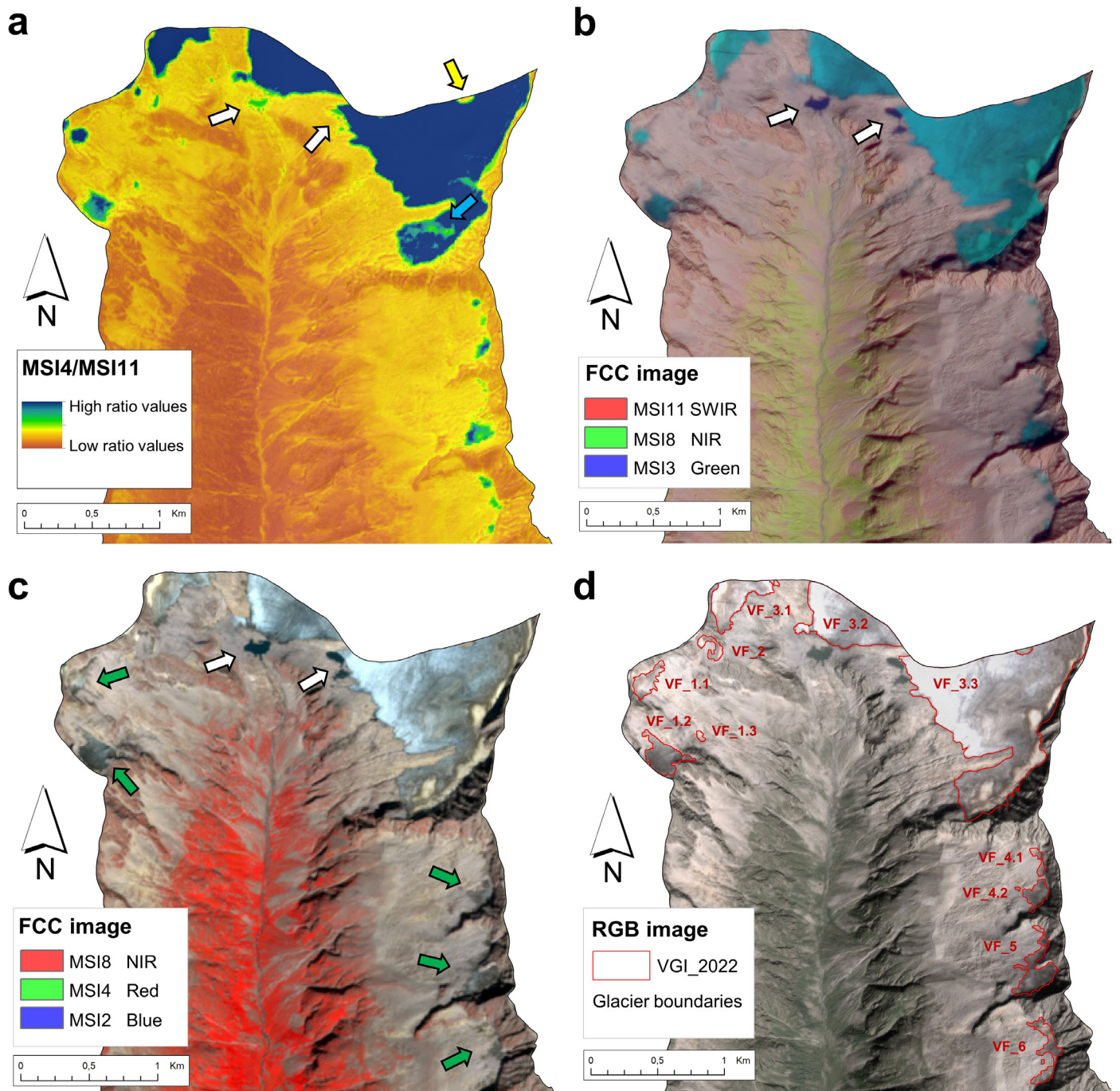


Fig. 2 - (a) MSI4/MSI11 band ratio. (b) MSI11, MSI8, MSI3 FCC image. (c) MSI8, MSI4, MSI2 FCC image. (d) Delineation of glacier boundaries for the elaboration of the VGI\_2022. White arrows indicate the presence of water bodies. The yellow arrow indicates the presence of a rocky outcrop. Green arrows indicate the presence of dirty ice above the glacier surface. The blue arrow shows some areas above glacier surface with slightly lower MSI4/MSI11 ratio values. Data source: S2B\_MSIL1C\_20220801T100559\_N0400\_R022\_T32TPS\_20220801T121930.

The MSI4/MSI11 ratio also highlights some objects characterised by medium-high values (Fig. 2a), which can be easily distinguished from glaciers as water bodies by analysing the MSI8/MSI11 ratio, as well as the FCC images (Paul et al., 2007). Indeed, Fig. 2b and Fig. 2c highlight the presence of three different proglacial lakes at north in contact with the VF\_3.2 and VF.3.3 glacial margin (Fig. 2d; i.e., ice-contact type; Cannone et al., 2008; Diolaiuti & Smiraglia, 2010). In both cases, lakes are represented with a dark blue colour that differs from the petrol green (Fig. 2b) and white-turquoise (Fig. 2c) of the glacier surfaces. Moreover, an

isolated rocky outcrop was observed below the VF\_3.3 ice-divide (Fig. 2a,d).

Nevertheless, debris-covered glacier parts were not emphasised by the band ratios because of their spectral similarity to surrounding terrain (Fig. 3a; Paul et al., 2007). Anyway, despite the quite similar colour of debris covering the ice with respect to that deposited on slopes and rocky outcrops, debris-covered glacier parts were detected by analysing the MSI2, MSI3, MSI4 and MSI8, MSI4, MSI2 FCC images (Fig. 3b). In fact, supraglacial debris can be easily distinguished due to its darker grey tone given

Table 2 - Data related to the twenty glaciers currently included in the Fumo Valley (VGI\_2022). The "NIGI" field refers to the "ID Code" of the New Italian Glacier Inventory (Smiraglia & Diolaiuti, 2015). Glaciers are classified according to the size classification proposed by Paul et al. (2004a,b).

The Vedretta di Fumo glacier (637; see Smiraglia & Diolaiuti, 2015) is subdivided into three distinct apophyses (VF\_3.1, VF\_3.2, VF\_3.3).

ID	NIGI	Name	Glacier type	Size class (km <sup>2</sup> )	Aspect
VF_1.1	614	Val di Fumo W	Mountain	< 0.1	SE
VF_1.2	614.1	Val di Fumo W I	Mountain	< 0.1	SE
VF_1.3	614.2	Val di Fumo W II	Glacieret	< 0.1	SE
VF_2	615	Val di Fumo Centrale	Glacieret	< 0.1	S
VF_3.1	637	Vedretta di Fumo	Mountain	< 0.1	E
VF_3.2				0.1-0.5	SW
VF_3.3				0.5-1	SW
VF_4.1	616	Corno di Cavento SW	Glacieret	< 0.1	W
VF_4.2				< 0.1	W
VF_5	617	Monte Folletto NW	Mountain	< 0.1	W
VF_6	618	Monte Folletto SW	Mountain	< 0.1	W
VF_7	619	Passo del Folletto W	Glacieret	< 0.1	W
VF_8.1	620	Caré Alto W	Glacieret	< 0.1	SW
VF_8.2	620.1	Caré Alto W I	Glacieret	< 0.1	SW
VF_9	621	Caré Alto SW	Glacieret	< 0.1	W
VF_10	624	Cop di Casa	Glacieret	< 0.1	S
VF_11	625	Cop di Breguzzo	Mountain	< 0.1	NW
VF_12	626	Cima Danerba	Glacieret	< 0.1	NW
VF_13	627	Cima Bissina N	Glacieret	< 0.1	N
VF_14	627.1	Cima Bissina N I	Glacieret	< 0.1	N

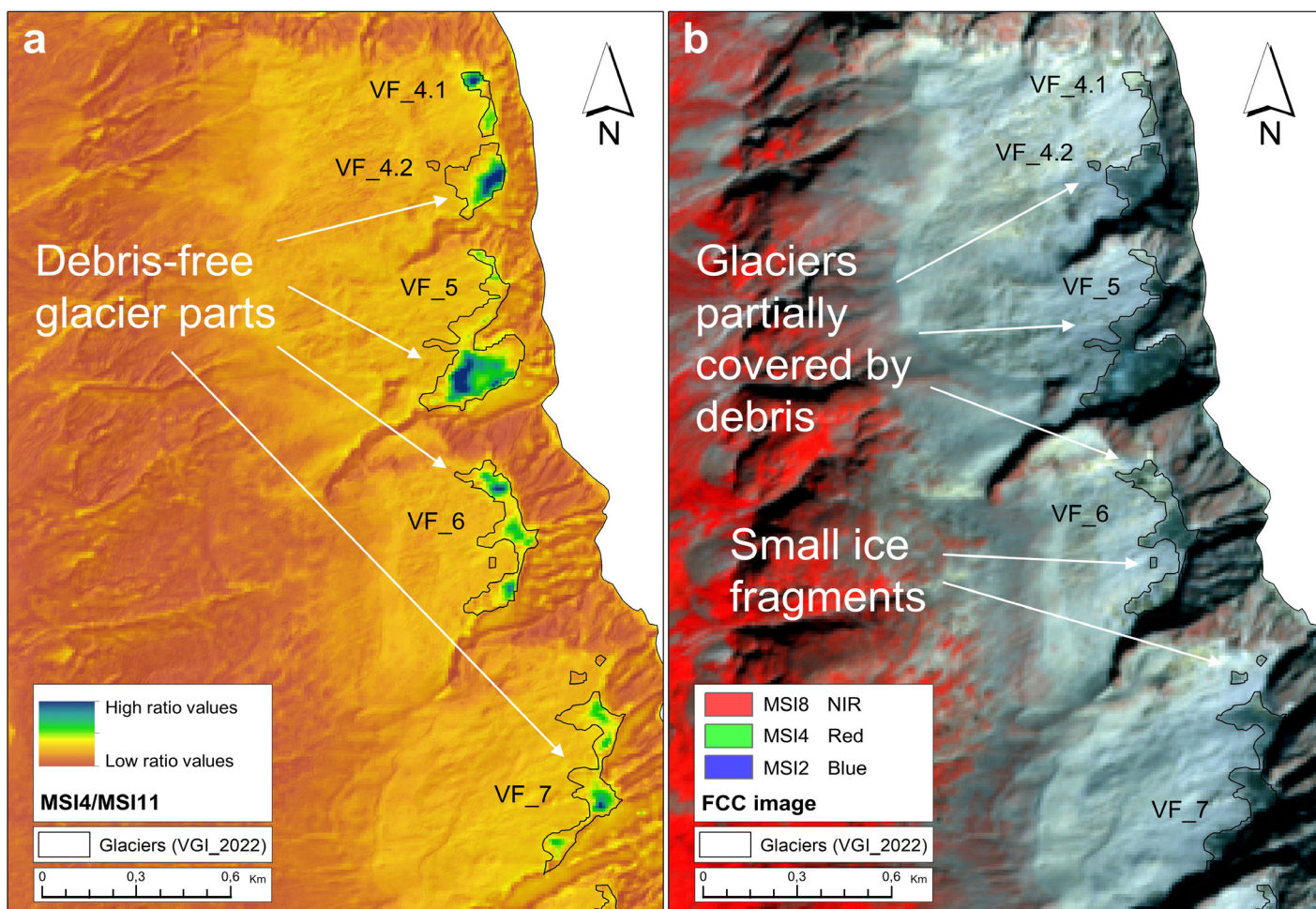


Fig. 3 - (a) Debris-free glacier parts emphasised by the MSI4/MSI11 band ratio with blue, light blue and green colours. (b) Glacier parts covered by debris and small ice fragments emphasised by the MSI8, MSI4, MSI2 FCC image. Data source: S2B\_MSIL1C\_20220801T100559\_N0400\_R022\_T32TPS\_20220801T121930.

by the higher humidity (Fea et al., 2013). Several small patches of fragmented ice remnants were also identified near the main glacial bodies (Fig. 3b). However, these ice fragments were not classified as individual glaciers due to their exiguous size (<0.005 km<sup>2</sup>). Thus, they were unified to the main glacial body closer to them (e.g., VF\_4.2, VF\_6 and VF\_7; Fig. 3b; Tab. 2).

Twenty glacial bodies were identified and included in the VGI\_2022 (Tab. 2). Sixteen of them are fully in the catchment (e.g., Fig. 4a,b,c). Glaciers are limitedly distributed at the valley head, as well as at higher elevations along the eastern catchment ridge. All of these glaciers were previously included in the NIGI (data referring to 2011; Smiraglia & Diolaiuti, 2015), even if some of them have recently been affected by fragmentation into distinct glacial bodies. The actual total glacier extent is 1.58 km<sup>2</sup> (Fig. 5). Vedretta di Fumo is the largest glacier in the study area (1.19 km<sup>2</sup>), belonging to the 1-2 km<sup>2</sup> size class (Paul et al., 2004a,b). It is subdivided into three distinct apophyses (VF\_3.1, VF\_3.2, VF\_3.3; Fig. 2d; Tab. 2). The eastern apophyses (VF\_3.2 and VF\_3.3) have an area of 0.20 and 0.90 km<sup>2</sup> respectively, while the western one has an area of 0.09 km<sup>2</sup> (Tab. 2; Tab. 3). The other glaciers belong to the < 0.1 km<sup>2</sup> size class (Paul et al., 2004a,b) (Tab. 2). According to Smiraglia & Diolaiuti (2015), six glaciers are classified as mountain glaciers, whereas the others are glacierets (Tab. 2). VF\_1.3 is <0.005 km<sup>2</sup>. Thus, it was classified as an “extinct glacier” with respect to the NIGI (Smiraglia & Diolaiuti, 2015, Tab. 3).

### Glacial variations from Little Ice Age to present

The comparison between glacier inventories related to different time periods was carried out in order to determine the variations in

terms of number of glaciers and glacierised surface in the Fumo Valley (D’Agata et al., 2014, 2018). Five different databases were compared to the VGI\_2022: LGI\_1850 (Zanoner et al., 2017), IGI\_1958 (CGI-CNR 1959, 1962), WGI\_1981 (Haeberli et al., 1989; WGMS & NSIDC, 1999), TGI\_2003, and TGI\_2015 (Fig. 5, Tab. 3; Fig. 6).

The total glacierised area related to LGI\_1850, IGI\_1958, WGI\_1981, TGI\_2003, and TGI\_2015 is respectively 8.44, 2.45, 4.32, 2.56, and 2.24 km<sup>2</sup> (Fig. 5). Likewise, the total number of glacial bodies is 18 (LGI\_1850), 11 (IGI\_1958), 18 (WGI\_1981), 16 (TGI\_2003), and 18 (TGI\_2015) (Fig. 5).

According to the size classification of Paul et al. (2004a,b), LGI\_1850 includes one glacier (Vedretta di Fumo) in the 2-5 km<sup>2</sup> class, two glaciers in the 1-2 km<sup>2</sup> class, two glaciers in the 0.5-1 km<sup>2</sup> class, six glaciers in the 0.1-0.5 km<sup>2</sup> class, and two glaciers in the <0.1 km<sup>2</sup> class. The IGI\_1958 includes one glacier in the 1-2 km<sup>2</sup> class, four glaciers in the 0.1-0.5 km<sup>2</sup> class, and six glaciers in the <0.1 km<sup>2</sup> class. The WGI\_1981 includes one glacier in the 1-2 km<sup>2</sup> class, eleven glaciers in the 0.1-0.5 km<sup>2</sup> class, and six glaciers in the <0.1 km<sup>2</sup> class. The TGI\_2003 includes one glacier in the 1-2 km<sup>2</sup> class, three glaciers in the 0.1-0.5 km<sup>2</sup> class, and the others in the <0.1 km<sup>2</sup> class. The TGI\_2015 includes one glacier in the 1-2 km<sup>2</sup> class, one glacier in the 0.1-0.5 km<sup>2</sup> class, and the others in the <0.1 km<sup>2</sup> class (Tab. 3; Tab. 4).

The IGI\_1958 includes ten glaciers classified as extinct with respect to LGI\_1850. The WGI\_1981 includes five glaciers classified as extinct with respect to LGI\_1850, five glaciers classified as active landforms in spite of they were classified as extinct in the IGI\_1958, and one glacier reported in the study area for the first

**Table 3 - Surface data related to the glacier inventories considered in the present study: LGI\_1850, IGI\_1958, WGI\_1981, TGI\_2003, TGI\_2015 and VGI\_2022. The “ID” field refers to the VGI\_2022 (Tab. 2). In some cases, glaciers have been merged together if they formed a single glacial body in the previous reference inventory. \* = data estimated by proportion between the Vedretta di Fumo (VF\_3) glacier surface in the IGI\_1958 and the entire Lobbia glacier surface in the IGI\_1958 and WGI\_1981 due to lack of data.**

ID	LGI_1850 Km <sup>2</sup>	IGI_1958 Km <sup>2</sup>	WGI_1981 Km <sup>2</sup>	TGI_2003 Km <sup>2</sup>	TGI_2015 Km <sup>2</sup>	VGI_2022 Km <sup>2</sup>
VF_1.1	0.91	0.18	0.18	0.09	0.07	0.03
VF_1.2				0.10	0.09	0.05
VF_1.3				0.02	0.02	extinct
VF_2	2.76	1.50	1.56*	0.03	0.03	0.02
VF_3.1				1.62	0.14	0.09
VF_3.2					1.32	0.20
VF_3.3						0.90
VF_4.1	1.02	0.20	0.37	0.08	0.09	0.01
VF_4.2						0.02
VF_5						0.15
VF_6	1.00	0.04	0.21	0.07	0.06	0.04
VF_7		0.07	0.29	0.16	0.09	0.05
VF_8.1	0.75	0.04	0.17	0.05	0.03	0.01
VF_8.2					0.01	0.01
VF_9					0.05	0.23
VF_10	0.07	extinct	0.07	0.03	0.02	0.02
VF_11	0.48	0.10	0.21	0.05	0.05	0.02
VF_12	0.15	0.08	0.11	0.05	0.04	0.02
VF_13	0.16	0.04	0.08	0.04	0.03	0.01
VF_14				0.01	0.01	0.01

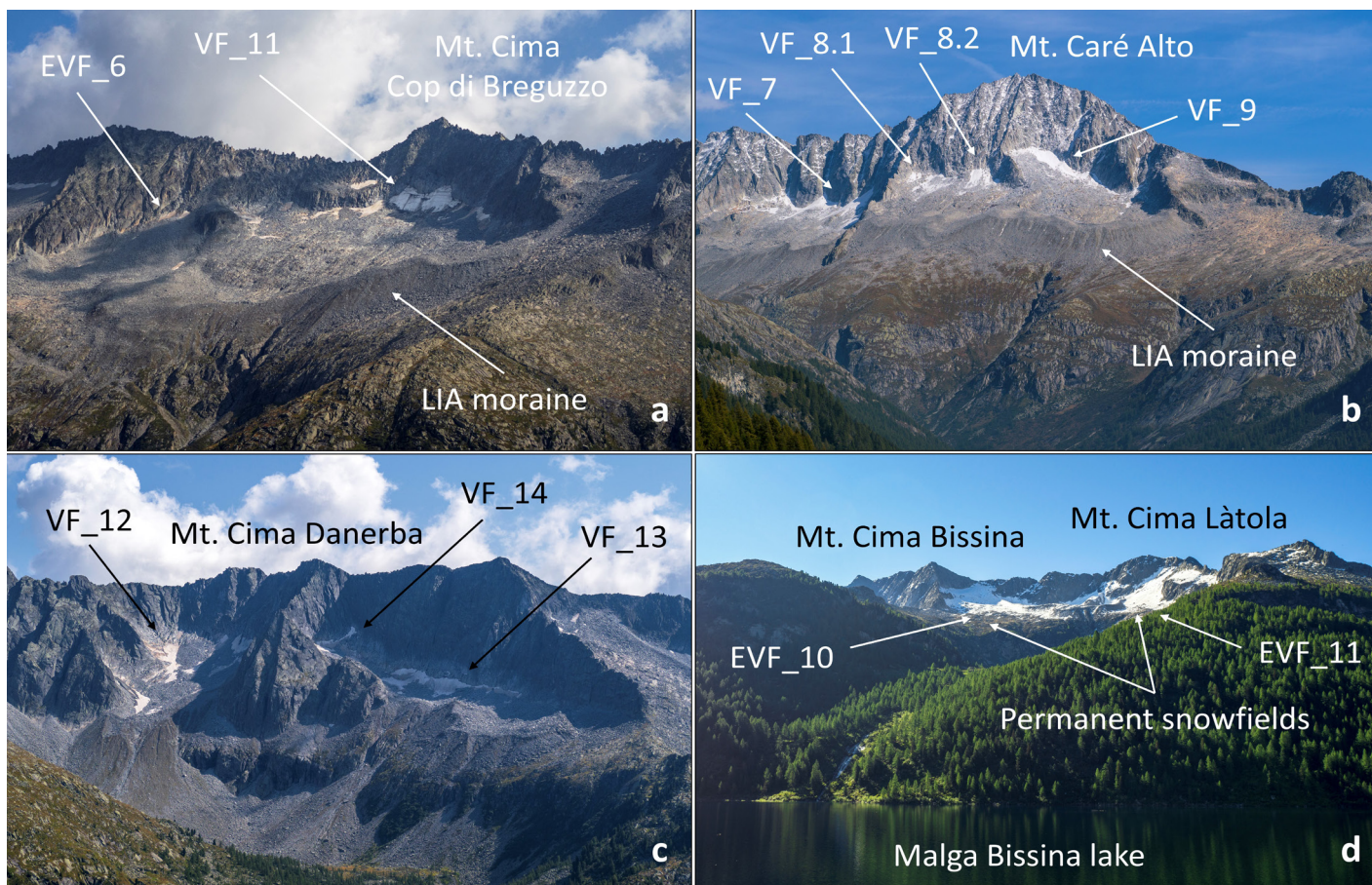


Fig. 4 - (a) Cop di Breguzzo glacier (VF\_11; photo taken on 14 September 2020). (b) Passo del Folletto W (VF\_7), Caré Alto W (VF\_8.1), Caré Alto W I (VF\_8.2) and Caré Alto SW (VF\_9) glaciers (photo taken on 01 October 2020). (c) Cima Danerba (VF\_12), Cima Bissina N (VF\_13) and Cima Bissina N I (VF\_14) glaciers (photo taken on 14 September 2020). (d) Permanent snowfields below Mt. Cima Bissina (2882 m a.s.l.) and Mt. Cima Låtola (2832 m a.s.l.) (photo taken on 22 June 2020). The figure shows the presence of debris that partially covers some of the glaciers.

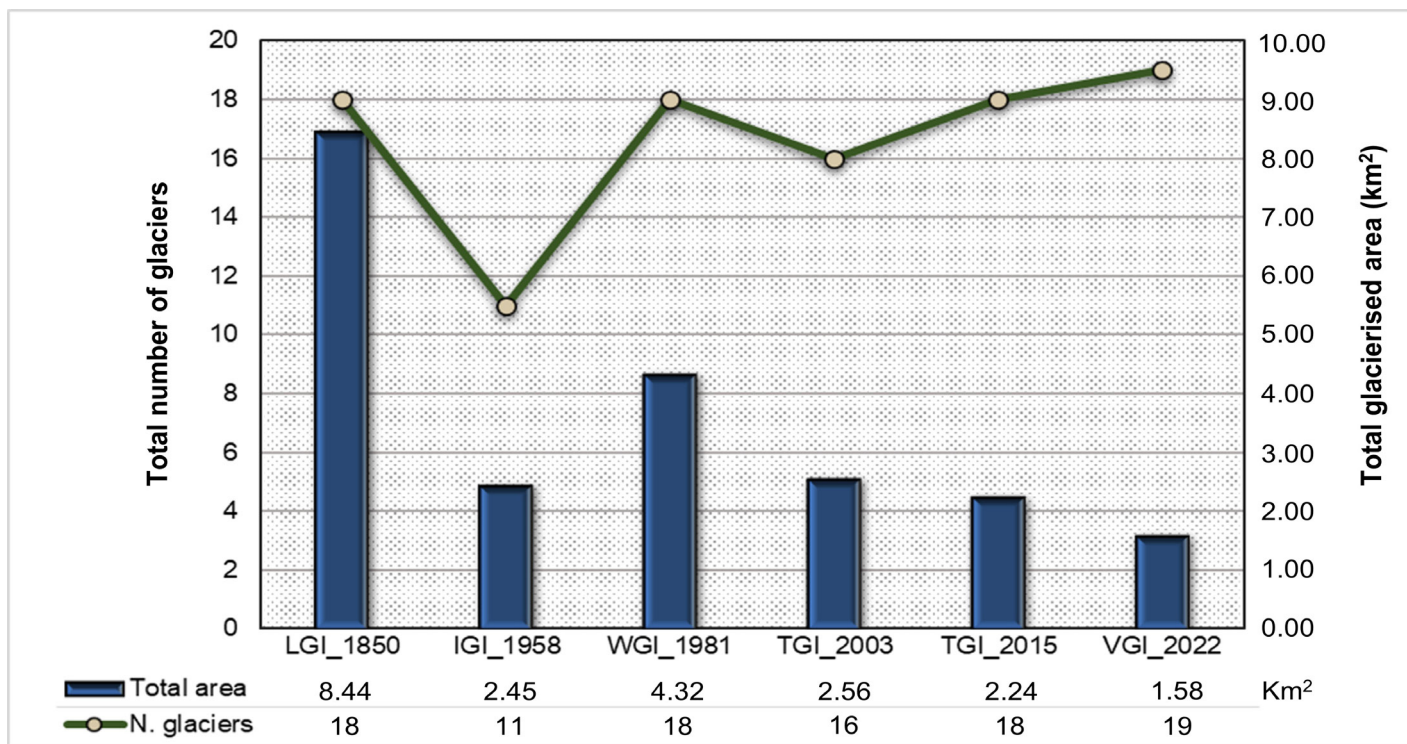


Fig. 5 - Total glaciated surface and total number of glaciers in the Fumo Valley. Data related to LGI\_1850, IGI\_1958, WGI\_1981, TGI\_2003, TGI\_2015 and VGI\_2022 glacier inventories.

**Table 4 - Surface data related to extinct glaciers after WGI\_1981. Glaciers are numbered and coded based on the maximum number of glacial bodies as in the WGI\_1981. Glaciers have been merged together if they formed a single glacial body in the previous reference inventory.**

ID	LGI_1850 Km <sup>2</sup>	IGI_1958 Km <sup>2</sup>	WGI_1981 Km <sup>2</sup>	TGI_2003 Km <sup>2</sup>	TGI_2015 Km <sup>2</sup>	VGI_2022 Km <sup>2</sup>
EVF_1	0.04	extinct	extinct	extinct	extinct	extinct
EVF_2	0.26	extinct	0.05	extinct	extinct	extinct
EVF_3			0.08	extinct	extinct	extinct
EVF_4	0.10	extinct	extinct	extinct	extinct	extinct
EVF_5	0.18	extinct	0.13	extinct	extinct	extinct
EVF_6	-	-	0.07	extinct	extinct	extinct
EVF_7	0.01	extinct	extinct	extinct	extinct	extinct
EVF_8	0.10	extinct	extinct	extinct	extinct	extinct
EVF_9	0.13	extinct	0.08	extinct	extinct	extinct
EVF_10	0.02	extinct	extinct	extinct	extinct	extinct
EVF_11	0.30	extinct	0.15	extinct	extinct	extinct

time (EVF\_6; Fig. 4a). The TGI\_2003 includes ten extinct glaciers that no longer underwent reactivation (Fig. 6; Tab. 4). Some extinct glaciers actually remain as permanent snowfields (e.g., EVF\_10 and EVF\_11; Fig. 4d).

The comparison between glacier surface data revealed a variation of -5.99 km<sup>2</sup> in 1850-1958, +1.87 km<sup>2</sup> in 1958-1981, -1.76 km<sup>2</sup> in 1981-2003, -0.32 km<sup>2</sup> in 2003-2015, -0.66 km<sup>2</sup> in 2015-2022, -6.86 km<sup>2</sup> in 1850-2022, -0.87 km<sup>2</sup> in 1958-2022, and -2.74 km<sup>2</sup> in 1981-2022 (Tab. 5). The percentage of variation is -71.0% in 1850-1958, +76.3% in 1958-1981, -40.7% in 1981-2003, -12.5% in 2003-2015, -29.5% in 2015-2022, -81.3% in 1850-2022, -35.5% in 1958-2022, and -63.4% in 1981-2022 (Tab. 5). The annual rate of variation is -0.7% yr<sup>-1</sup> in 1850-1958, +3.3% yr<sup>-1</sup> in 1958-1981, -1.9% yr<sup>-1</sup> in 1981-2003, -1.0% yr<sup>-1</sup> in 2003-2015, -4.2% yr<sup>-1</sup> in 2015-2022, -0.5% yr<sup>-1</sup> in 1850-2022, -0.6% yr<sup>-1</sup> in 1958-2022, and -1.5% yr<sup>-1</sup> in 1981-2022 (Tab. 5).

VF\_1.1, VF\_1.2 and VF\_1.3 glaciers constitute three different glacial units derived from the fragmentation of a glacial diffuence

of the Adamello/Mandrone glacier (Smiraglia & Diolaiuti, 2015; Tab. 2). In the IGI\_1958 and WGI\_1981 the three glaciers were a single glacial body belonging to the 0.1-0.5 km<sup>2</sup> size class (Tab. 3), while in the TGI\_2003 they were already three distinct glaciers. In the VGI\_2022, VF\_1.3 is classified as extinct (<0.005 km<sup>2</sup>), whereas VF\_1.1 and VF\_1.2 extend for <0.1 km<sup>2</sup> (Tab. 3).

VF\_2, VF\_3.1, VF\_3.2 and VF\_3.3 glaciers constitute a diffuence of the Lobbia glacier (Smiraglia & Diolaiuti, 2015). In the TGI\_2003 the Vedretta di Fumo glacier (VF\_3.1, VF\_3.2, and VF\_3.3; Tab. 2) was a single glacial body, while between TGI\_2003 and TGI\_2015 glacier shrinkage caused the formation of two distinct apophyses (Tab. 3). In the VGI\_2022 the eastern apophysis tongue has separated into two distinct glacial bodies below the ice-divide (Baroni & Carton, 1990a) (Fig. 6). Furthermore, the newly formed proglacial lakes and the isolated rocky outcrop (Fig. 2), are located on surfaces that were covered by ice in the TGI\_2015 (Fig. 6).

All the small glaciers experienced a marked expansion between IGI\_1958 and WGI\_1981 (Tab. 3), apart from the aforementioned

**Table 5 - Total surface variation (in terms of area and percentage of variation) and total rate of variation per year of the Fumo Valley glaciers in the following temporal ranges: 1850-1958, 1958-1981, 1981-2003, 2003-2015, 2015-2022, 1850-2022, 1958-2022 and 1981-2022.**

Total variation 1850-1958 (km <sup>2</sup> )	- 5.99 ↓	Total variation 1958-1981 (km <sup>2</sup> )	+1.87 ↑
Total variation 1981-2003 (km <sup>2</sup> )	- 1.76 ↓	Total variation 2003-2015 (km <sup>2</sup> )	- 0.32 ↓
Total variation 2015-2022 (km <sup>2</sup> )	- 0.66 ↓	Total variation 1850-2022 (km <sup>2</sup> )	- 6.86 ↓
Total variation 1958-2022 (km <sup>2</sup> )	- 0.87 ↓	Total variation 1981-2022 (km <sup>2</sup> )	- 2.74 ↓
Total variation 1850-1958 (%)	- 71.0 ↓	Total variation 1958-1981 (%)	+76.3 ↑
Total variation 1981-2003 (%)	- 40.7 ↓	Total variation 2003-2015 (%)	- 12.5 ↓
Total variation 2015-2022 (%)	- 29.5 ↓	Total variation 1850-2022 (%)	- 81.3 ↓
Total variation 1958-2022 (%)	- 35.5 ↓	Total variation 1981-2022 (%)	- 63.4 ↓
Rate of variation per year 1850-1958 (% yr <sup>-1</sup> )	- 0.7 ↓	Rate of variation per year 1958-1981 (% yr <sup>-1</sup> )	+3.3 ↑
Rate of variation per year 1981-2003 (% yr <sup>-1</sup> )	- 1.9 ↓	Rate of variation per year 2003-2015 (% yr <sup>-1</sup> )	- 1.0 ↓
Rate of variation per year 2015-2022 (% yr <sup>-1</sup> )	- 4.2 ↓	Rate of variation per year 1850-2022 (% yr <sup>-1</sup> )	- 0.5 ↓
Rate of variation per year 1958-2022 (% yr <sup>-1</sup> )	- 0.6 ↓	Rate of variation per year 1981-2022 (% yr <sup>-1</sup> )	- 1.5 ↓

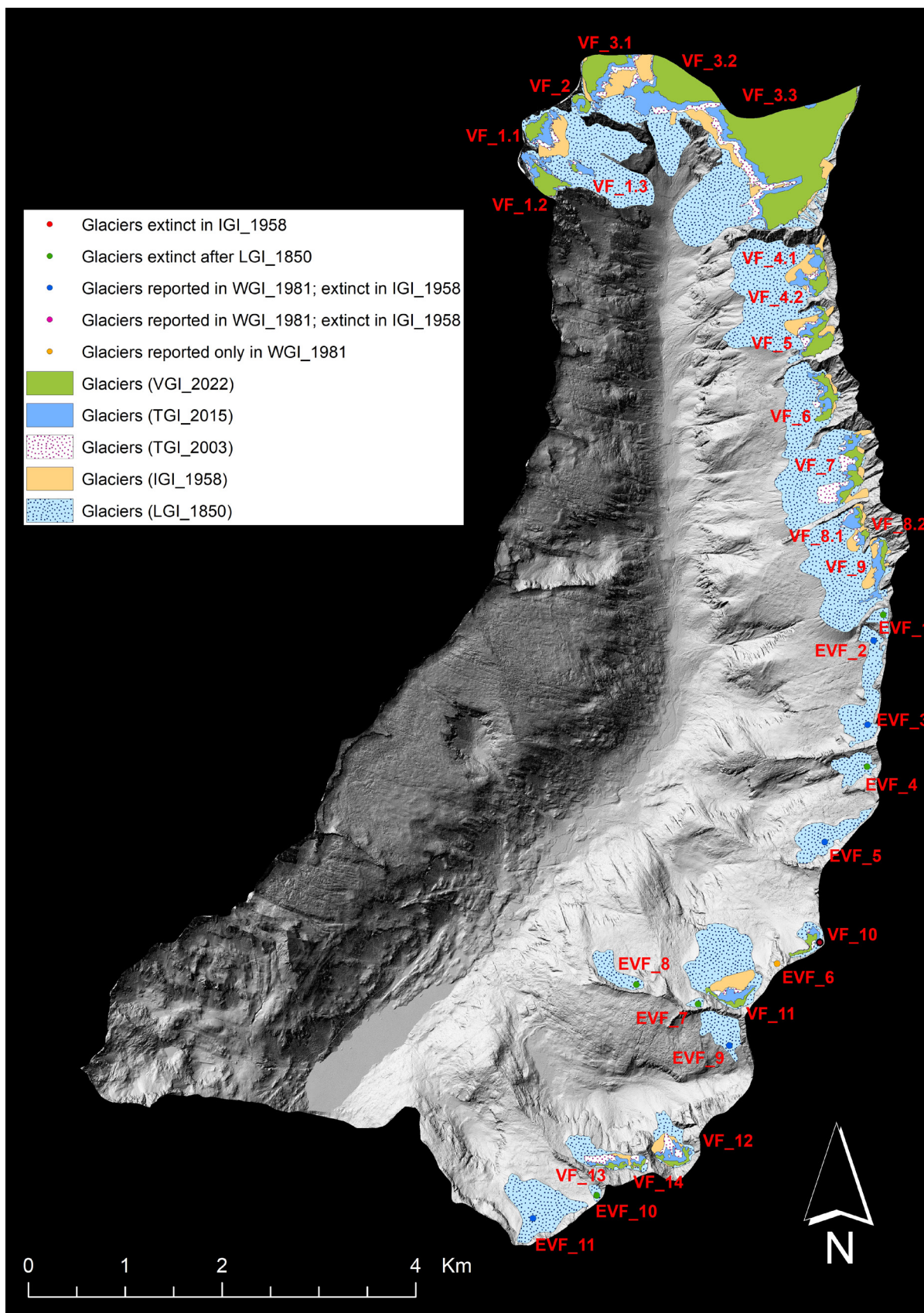


Fig. 6 - Localisation and extent of Fumo Valley glaciers as reported in the following glacier inventories: LGI\_1850; IGI\_1958; TGI\_2003; TGI\_2015; VGI\_2022 (Tab. 3; Tab. 4). Regarding WGI\_1981, the localisation of glaciers reported in Tab. 4 are represented. Glacier ID labels refer to VGI\_2022 (Tab. 2). LGI\_1850 shapefile data are derived from the Glaciers and Little Ice Age Hazard Map of the APT; for further details, see [Zanoner et al. \(2017\)](#). IGI\_1958 shapefile data are derived from [Bertoni & Casarotto \(2015\)](#). WGI\_1981 shapefile data are provided by WGMS & NSIDC (1999) (<https://www.nsidc.org/home>). TGI\_2003 and TGI\_2015 shapefile data are provided by the Prevention and Risk Service, APT (<http://www.territorio.provincia.tn.it/>). Map background: hillshade relief map derived from LiDAR DTM 2014 (© APT - Portale Geocartografico Trentino; [www.territorio.provincia.tn.it/](http://www.territorio.provincia.tn.it/)).

reactivation of some glaciers which were previously classified as extinct (Tab. 4). After this period, they experienced a regression phase (Fig. 5), which was followed, in some cases, by fragmentation (VF\_8.1, VF\_8.2, VF\_13, and VF\_14; Tab. 3) and by the downgrade to the lowest size class (VF\_5, VF\_7, VF\_11, and VF\_12; Tab. 3). Between TGI\_2015 and VGI\_2022 some glaciers underwent partial breakdown into smaller ice patches and fragments (VF\_6, VF\_7; Fig. 3).

**Temperature climatological data for the period 1991-2020**

The climate at Malga Bissina weather stations (T0156 and T0373; Tab. 1) in the thirty-year period 1991-2020 is attributable to the Cfc Köppen-Geiger climate type, which is characterised by humid temperate conditions, well-defined summer and winter seasons, and precipitation distributed during the whole year (without dry season) (Kottek et al., 2006). In particular, the MAAT is 5.1°C (Fig. 7). August is the hottest month (MMAT of 13.8°C), while January and February are the coldest months (MMAT of - 2.3°C) (Fig. 7). The MAmT is 0.4 °C (Fig. 7); February has the lowest MMmT (-7.7°C), while August has the highest MMmT (9.0°C). The MAMT is 9.8°C (Fig. 7); January has the lowest MMMT (2.7°C), while July has the highest MMMT (18.6°C). The mean seasonal temperatures are - 1.9°C in winter, 3.6°C in spring, 12.9°C in summer, and 5.8°C in autumn (Fig. 8). The mean minimum and maximum seasonal

temperatures are respectively -6.7 and 2.9°C in winter, -1.4 and 8.7°C in spring, 7.9 and 17.9°C in summer, and 1.8 and 9.8°C in autumn (Fig. 8).

The altitudinal climatic belts were calculated by applying the average thermal vertical gradient (0.59°C/100 m; Baroni et al., 2004) to the monthly and annual temperature normals (data not shown). The Cfc Köppen-Geiger climate type is compatible with an altitudinal range varying from 1770 to 1910 m a.s.l. From 1910 to 2430 m of altitude the climate is attributable to the Dfc Köppen-Geiger climate type (humid boreal climate of the Alpine tundra) with a mean temperature of the coldest months (January and February) ≤ - 3°C and > - 38°C, and at least 1-3 months with mean temperatures > 10°C (Kottek et al., 2006). Above 2430 m of altitude, the climate is attributable to the ET Köppen-Geiger climate type (Alpine polar climate), which is characterised by a mean temperature of the hottest month (August) < 10 and ≥ 0°C (Kottek et al., 2006). The mean annual isotherms of 0, -1 and -2°C lie respectively at 2654, 2824 and 2993 m a.s.l.

**Temperature climatological data for the period 1971-2000**

The MAAT at Malga Bissina weather station (T0156; Tab. 1) during the thirty-year period 1971-2000 is 4.5°C (Fig. 9). August is the hottest month (MMAT of 12.7°C), while February is the coldest month (MMAT of - 2.6°C) (Fig. 9). The MAmT is 0.3 °C

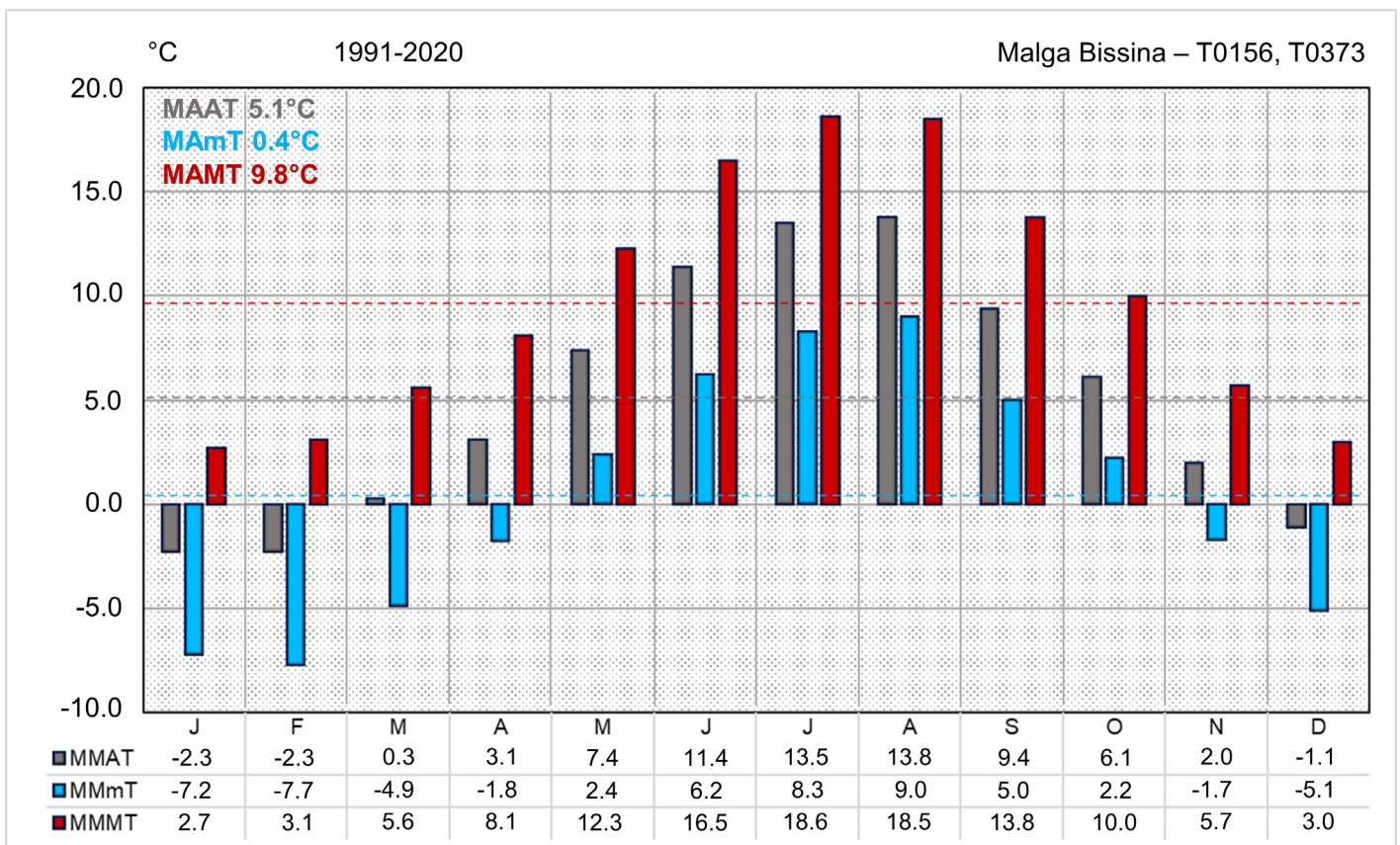


Fig. 7 - Standard normals of temperature data related to the thirty-year period 1991-2020. MMAT = mean monthly air temperature; MAAT = mean annual air temperature; MMmT = mean monthly minimum air temperature; MAmT = mean annual minimum air temperature; MMMT = mean monthly maximum air temperature; MAMT = mean annual maximum air temperature. The temperature data are related to Malga Bissina weather stations T0156 and T0373 (Tab. 1).

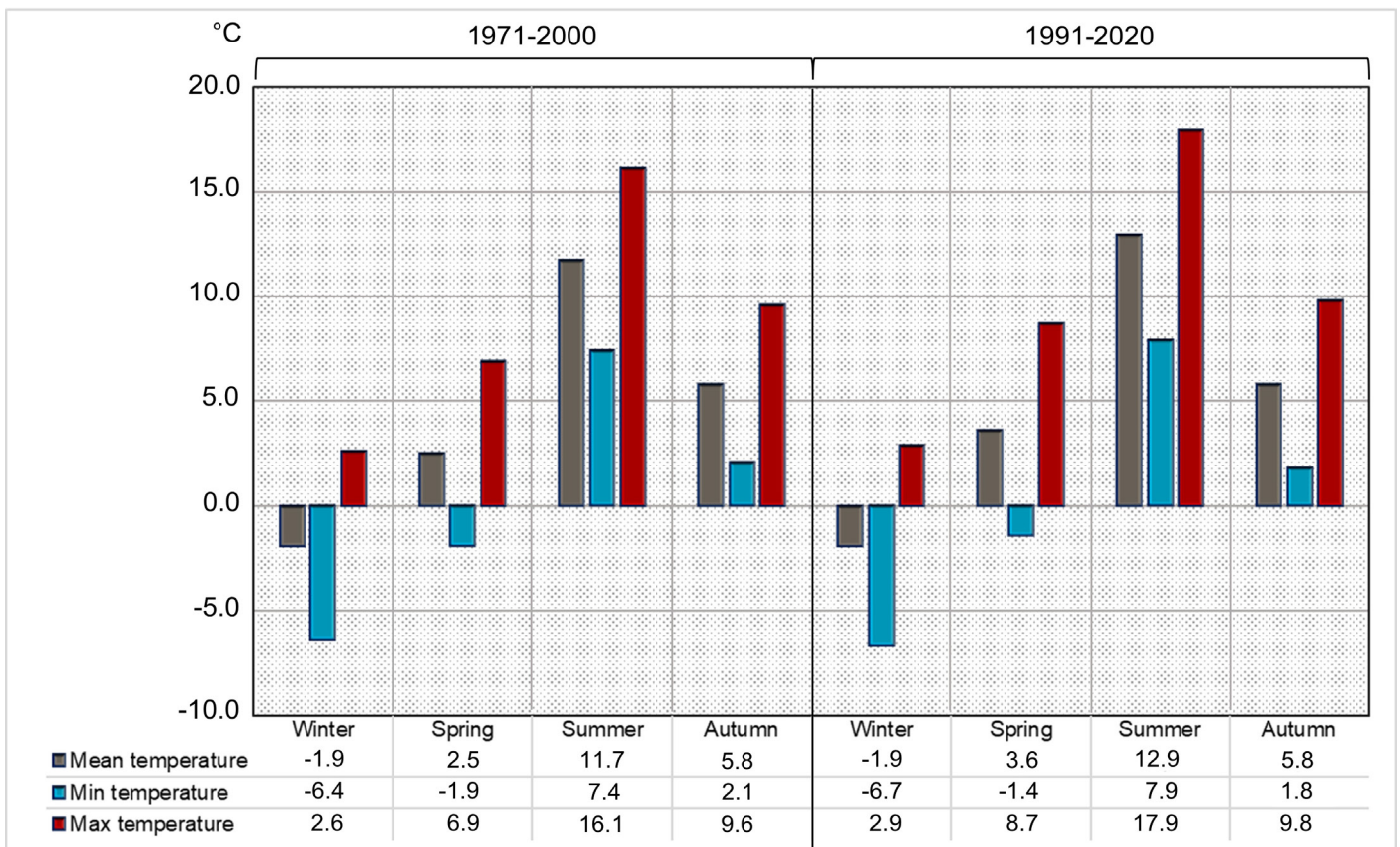


Fig. 8 - Standard seasonal normals related to 1971-2000 and 1991-2020 thirty-year periods. The temperature data are related to Malga Bissina weather stations T0156 and T0373 (Tab. 1).

(Fig. 9); February has the lowest MMmT (-7.8°C), while August has the highest MMmT (8.5°C). The MAMT is 8.8°C (Fig. 9); January has the lowest MMT (2.2°C), while July has the highest MMT (17.2°C). The mean seasonal temperatures are -1.9°C in winter, 2.5°C in spring, 11.7°C in summer, and 5.8°C in autumn (Fig. 8). The mean minimum and maximum seasonal temperatures are respectively -6.4 and 2.6°C in winter, -1.9 and 6.9°C in spring, 7.4 and 16.1°C in summer, and 2.1 and 9.6°C in autumn (Fig. 8).

The Cfc Köppen-Geiger climate type is compatible with an altitudinal range varying from 1790 to 1860 m a.s.l. From 1860 to 2240 m of altitude, the climate is attributable to the Dfc Köppen-Geiger climate type. Above 2240 m of altitude the climate is attributable to the ET Köppen-Geiger climate type (Kottek et al., 2006). The mean annual isotherms of 0, -1 and -2°C lie respectively at 2553, 2722 and 2890 m a.s.l.

## DISCUSSION

During the LIA, the extent of the Fumo Valley glaciers (8.44 km<sup>2</sup>; Fig. 5) was equal to 17.60% of the total glacierised area in the Adamello Group (i.e., 47.95 km<sup>2</sup>; Zanoner et al., 2017). Glaciers in the study area have experienced a phase of considerable retreat since the end of the LIA (Fig. 5; Fig. 6; Orombelli et al., 2011), with the consequent disappearance of several small isolated glacial bodies, as observed for all the Italian glacierised areas (see Salvatore et al., 2015). As demonstrated by several studies (e.g.,

Giaccone et al., 2015 and Colombo et al., 2016) new geomorphic systems driven by the morphoclimatic readjustment develop during glacial retreat periods. For instance, Zanoner et al. (2017) reported that in the Adamello Group LIA and post-LIA glacial deposits extend for 9.65 km<sup>2</sup>. These geomorphic systems require special attention in geomorphological hazard management (Chiarle & Mortara, 2008), since poorly consolidated glacial deposits related to glacier forelands and paraglacial environments are frequently subjected to degradation and instability processes, triggering debris flows, cryonival processes and other mass-wasting phenomena (Deline et al., 2015).

The total area reduction experienced by the Fumo Valley glaciers between 1958 and 2022 (-0.87 km<sup>2</sup>, equal to -35.5%; Tab. 5) is comparable to other studies carried out at national scales (see Smiraglia & Diolaiuti, 2015; Smiraglia et al., 2015). However, the glacial progression phase observed in the study area between 1958 and 1981 (Fig. 5; Tab. 3) also agrees with the positive trend observed for the total Italian glacierised area during the same period, i.e., from ~ 527 km<sup>2</sup> in the IGI (CGI-CNR, 1959) to ~ 608 km<sup>2</sup> in the WGI (Haeberli et al., 1989). This evidence could be partially ascribed to the different methods used for the elaboration of the two inventories. For instance, Belloni et al. (1985) stated that in both inventories surface data may be subjected to lower accuracy than other recorded parameters, despite the data reported in the WGI are generally more reliable than those reported in the IGI. Furthermore, the aerial photos used

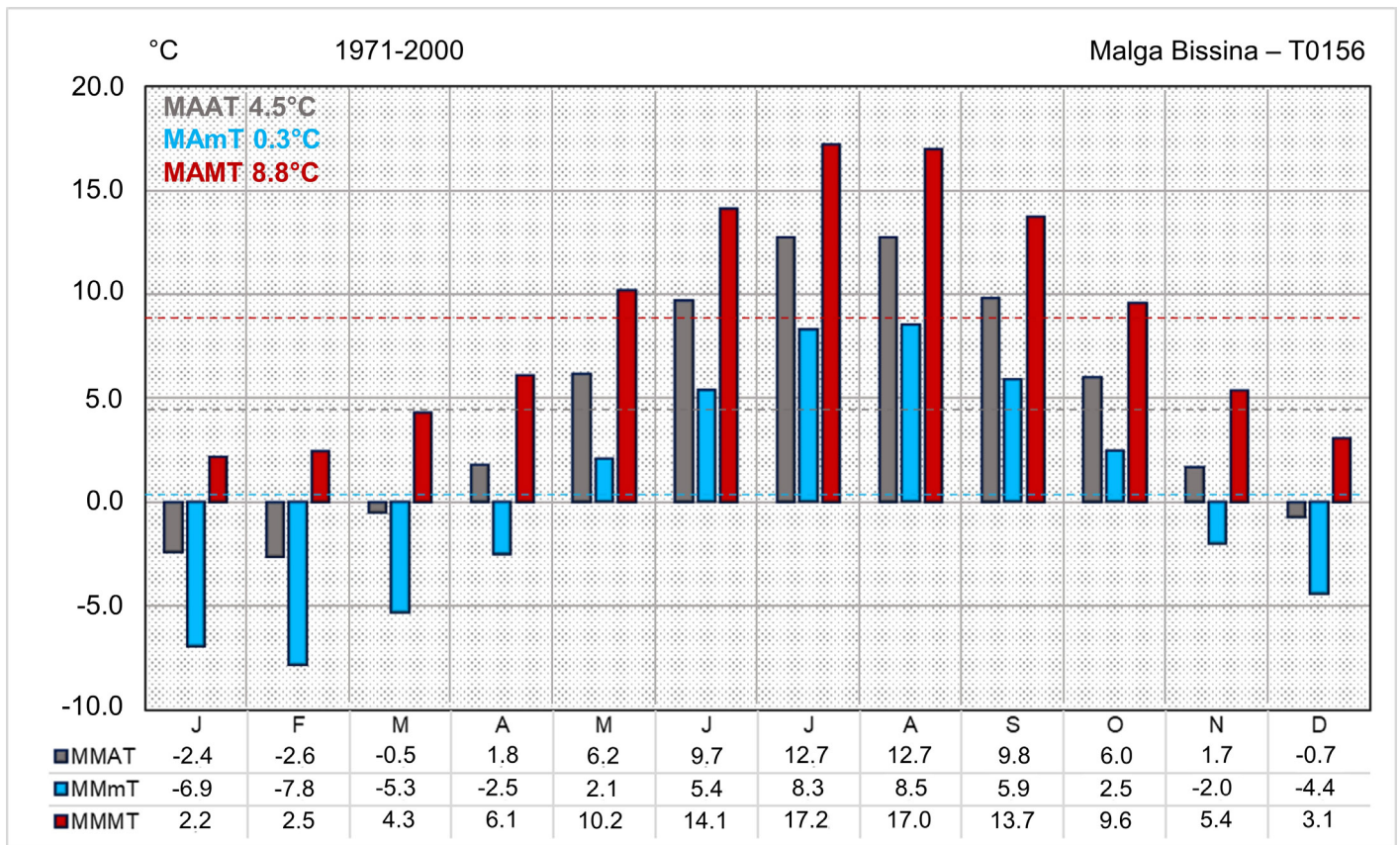


Fig. 9 - Standard normals of temperature data related to the thirty-year period 1971-2000. MMAT = mean monthly air temperature; MAAT = mean annual air temperature; MMmT = mean monthly minimum air temperature; MAMt = mean annual minimum air temperature; MAMT = mean monthly maximum air temperature; MAMT = mean annual maximum air temperature. The temperature data are related to the Malga Bissina weather station T0156 (Tab.1).

for the acquisition of data related to the Italian glaciers within the WGI were affected by a non-negligible snow cover (Smiraglia et al., 2015; Diolaiuti et al., 2019). Therefore, snow cover could have biased the assessment of the glacierised surface. Nonetheless, the resulted increase in glacierised surface between 1958 and 1981 may partially be explained by the acknowledged glacier readvance episode occurred between the 1970s and 1980s in the Italian Alps (Citterio et al., 2007; Chiarle & Mortara, 2008; Salvatore et al., 2015). This phase culminated in the early 1980s with more than 80% of measured glaciers in the Adamello-Presanella Group in progression (Zanon, 1985).

Moreover, the WGI\_1981 reported some active glacierets which were previously classified as extinct in the IGI\_1958 (Fig. 6; Tab. 4). This fact may be explained by the regeneration of snowfields and small ice patches thanks to the imposition of climatic conditions more favourable to the glacial environment. Afterwards, these glacierets disappeared again and, in some cases, evolved into semi-permanent snowfields or other periglacial landforms (Fig. 4d). However, the WGI database unified data from snowfields and glacierets into the same category (see Müller et al., 1977) and, thus, it is not specified if these glacial units were actually glaciers. Hence, this evidence could explain why some of these small snowfields and glacierets were not included in the IGI, as suggested by Serandrei-Barbero & Zanon (1993). Thus, the total glacial surface in the WGI\_1981 (Fig. 5) could have been overestimated. Besides, after this phase, the Fumo Valley

glaciers have followed the trend inversion which is affecting the Alpine region due to the decrease of snowy precipitation and the constant increase of air temperature (Citterio et al., 2007; Diolaiuti et al., 2011).

The analysis of temperature data revealed evidence of warming air temperature at local scale between 1971-2000 and 1991-2020 thirty-year periods (+0.6°C in MAAT; Fig. 7; Fig. 9). Moreover, the increase in MAMT (+1°C) is higher than MAMt (+0.1°C). Also, the results highlight an average increase in MMAT higher in spring and summer than in autumn and winter (Fig. 8), as already pointed out by Di Piazza & Eccel (2012) for the Trentino province. More in detail, the seasonal temperature variation between the two periods exhibits a higher average absolute deviation in maximum temperatures (i.e., 0.4°C in winter, 1.8°C in spring and summer, and 0.3°C in autumn) than minimum temperatures. On the contrary, the latter show a more swinging trend between positive and negative variations with respect to null deviation, showing greater homogeneity in mean seasonal deviations (i.e., around 0.3-0.5°C). Therefore, the air warming is more pronounced in summer and spring, as already observed in the European Alps (see Auer et al., 2007; EEA, 2009; Hock et al., 2019). Moreover, these results not only show that the increase in the average temperature values is heavily biased towards maximum temperatures but also that the latter show less homogeneity in average seasonal variations. Anyway, since atmospheric warming is the main driving factor of the generalised

glacier recession (Hock et al., 2019), the obtained results may be correlated with the glacier surface reduction observed between 1981 and 2022.

Both percentage and annual rate of variation of the Fumo Valley glaciers in the 1981-2003 period (1.9% yr<sup>-1</sup>, -40.7%) likely depend on the total glacierised area reported in the WGI\_1981. Thus, these results may be affected by overestimation. Instead, the annual rate of variation between 2003 and 2015 (-1.0% yr<sup>-1</sup>) is roughly the same value as for the Adamello Group, that is, -1.25% yr<sup>-1</sup> between 2003 and 2013 (Bertoni & Casarotto, 2015). However, between 2015 and 2022 glaciers in the study area lost approximately 30% of their total area, with an increase in the annual rate of variation (-4.2% yr<sup>-1</sup>). Despite the intrinsic uncertainties in delimiting glacial boundaries, mostly due to the resolution of S2 image bands (i.e., 10 m; Drusch et al., 2012), the evidence of glacier fragmentation, tongue separation, as well as the formation of proglacial lakes and rocky outcrops above glacier surface (Fig. 2a; Fig. 3a,b), probably suggest a worsening of cryosphere degradation between 2015 and 2022 (see Paul et al., 2007; Chiarle & Mortara, 2008; Diolaiuti & Smiraglia, 2010). This phenomenon could be driven by positive feedbacks that have accelerated glacier shrinkage once it initiated. These feedbacks may further accelerate future glacier decline (e.g., thermokarst processes leading rapid further growth of proglacial lakes due to increasing ice melting), as already observed in the Adamello Group (i.e., in Lombardy sector; Maragno et al., 2009) and in other Alpine glacierised areas (e.g., Swiss Alps; Paul et al., 2007).

In addition, severe glacier shrinkage induced by increasing climate warming may have further contributed to an increase in supraglacial debris cover (Fig. 4a,b,c; D'Agata et al., 2020). Generally, this phenomenon is enhanced by the rate of mobilised debris input either from frost shattering, bedrock degradation processes or debultrussing of adjacent rock walls (Diolaiuti & Smiraglia, 2010). As stated by Nicholson et al. (2018), this fact could be relevant in a glacial environment degradation scenario, as debris cover generally influences the ablation rate by regulating the heat flux from surface to glacier ice, thus, influencing the glacier response to climate change (see also Azzoni et al., 2018).

Between 2003 and 2022 the total number of glaciers has progressively increased, from 16 in the TGI\_2003 to 19 in the VGI\_2022 (Fig. 5). This trend is likely explained by the degradation and subsequent fragmentation of unitary glacial units due to glacier shrinkage (Fig. 6; Brahmhatt et al., 2015), as already assessed in the Alpine region (Salvatore et al., 2015; Smiraglia & Diolaiuti, 2015).

The greatest surface loss is the one affecting the Vedretta di Fumo glacier, with a much higher surface variation than other small glaciers (Tab. 3). This evidence is likely explained by the unequal geometric features of the former compared to all the smaller glacial bodies. Thus, it couldn't be attributable to a higher susceptibility of the Vedretta di Fumo glacier. In fact, small glaciers experienced a higher percentage and annual rate of variation than the Vedretta di Fumo glacier. Moreover, all of them shifted towards the lowest size class in the TGI\_2015 (i.e., <0.1 km<sup>2</sup>; Paul et al., 2004a,b; Tab. 3). As already pointed out by other authors, small glaciers are more susceptible to climatic variations

on decennial time scale due to the faster reaction time than greater glacial bodies (Cannone et al., 2008; Orombelli, 2011), generally causing a greater percentage of surface reduction (Paul et al., 2004b; Bocchiola & Diolaiuti, 2010). Thus, considering the geometric features of these small glacial bodies, in the next decades they may almost completely disappear (as already happened for VF\_1.3; Tab. 3; Zemp et al., 2006).

Glaciers constitute a fundamental resource within a glacial hydrological regime, as they provide the main contribution of freshwater resources (Diolaiuti & Smiraglia, 2010), ensuring the minimum vital outflow within the catchment. The climatic variations that affect the water supply of small Alpine catchments such as the Fumo Valley are a critical control factor over the flow rates involved in the generation of hydroelectric power (Viviroli & Weingartner, 2004; Brown et al., 2006). On the one hand, following the progressive increase in Alpine cryosphere degradation, an increase in the water supply is expected in the short term. On the other hand, in the long term the disappearance of small glacial bodies may cause a progressive decrease in glacier runoff water flows (Haeberli et al., 2007; D'Agata et al., 2018). Therefore, the adaptation strategies to climate change will be crucial for an effective response to socio-economic challenges, as well as for the sustainable development of mountain communities (Grossi et al., 2013; Jones et al., 2019).

The analysis of temperature data revealed an altitudinal shift towards higher elevations of the mean annual isotherms of 0, -1 and -2°C of about 100 metres between the 1971-2000 and 1991-2020 periods. In the Central Alps, a MAAT of -1/-2°C approximately defines the lower limit for intact rock glaciers, which in turn is used as indicator of the present lower boundary of Alpine (discontinuous) permafrost (Guodong, 1983; Baroni et al., 2004; Guglielmin et al., 2022). Despite permafrost distribution is controlled by several factors on local scale, such as particular topographic and microclimatic features, the results imply a vertical altitudinal shift in permafrost climatic conditions (see also Colombo et al., 2016). This could have potential consequences for what concerns the hydrological role of permafrost (Jones et al., 2009), as well as directly or indirectly influencing ecosystem changes and the frequency of slope instability processes due to permafrost degradation (Chiarle & Mortara, 2008; Harris et al., 2009; Schoeneicht et al., 2011). However, Baroni et al. (2004) obtained strong evidence suggesting that intact rock glaciers couldn't be in equilibrium with present climatic conditions in the Adamello-Presanella Group. Moreover, they stated that the MAAT of -1/-2°C probably does not reflect steady-state conditions of intact rock glaciers in the Adamello-Presanella Group (i.e., since the lower limit of intact rock glaciers lies at approximately 2500 m a.s.l. while the mean annual isotherms of -1/-2°C lie at 2740 and 2910 m a.s.l.; Baroni et al., 2004). Therefore, Baroni et al. (2004) suggested that the MAAT must be used with caution in defining the lower limit of permafrost distribution in this regional context.

The rise in air temperature also determined a shift of altitudinal limits defining the boreal climate belt towards higher elevations (i.e., from 1860-2240 m a.s.l. in the 1971-2000 period to 1910-2430 m a.s.l. in the 1991-2020 period). Predictably, the Alpine polar climate belt lower limit moved from 2240 m a.s.l. to 2430

m a.s.l. According to future climate scenarios (see, e.g., Rubel et al., 2017), this evidence suggests a further altitudinal transition of the ecological conditions linked to the boreal and Alpine tundra climates in the next decades. This may result in the imposition of temperate conditions even at higher elevations, highly influencing ecosystem dynamics (Colombo et al., 2016).

## CONCLUSION

The results highlight a strong reduction in glacier coverage from the end of the LIA until the present time. Between 1958 and 2022 a total area reduction was observed, which is comparable to other studies carried out at national scales (Smiraglia et al., 2015). However, a minor progression phase occurred between 1958 and 1981, which may be partially due to the glacial readvance episode registered between the 1970s and 1980s in the Italian Alps (Salvatore et al., 2015). After this phase, the total glacial area has decreased following the general trend caused by the worsening of climatic conditions, as already recorded in the Alpine Region (Citterio et al., 2007; Diolaiuti et al., 2011).

An increase in air temperature occurred between the 1971-2000 and 1991-2020 periods, with a greater variation in the MAMT compared to MAmT, and a higher average temperature increase during spring and summer than in autumn and winter. These results are strong evidence of climatic changes occurring at local scale and agree with previous studies carried out at regional scale (Di Piazza & Eccel, 2012). Moreover, the altitudinal climate belts and the mean annual isotherms of 0, -1 and -2°C shifted towards higher elevations. This evidence may suggest an imposition of temperate climatic conditions at higher altitudes, as well as the potential degradation of periglacial environments and changes in permafrost climatic conditions.

In the more recent temporal range (2015-2022), an accelerated glacier shrinkage has been observed compared to the previous one (2003-2015), as suggested by higher annual variation rate, formation of ice-contact lakes, severe glacier fragmentation, tongue separation of the Vedretta di Fumo glacier, and extinction of one glacier. This evidence can be interpreted as truthful indicators of the impact of climate changes on the Alpine cryosphere (Diolaiuti & Smiraglia, 2010; D'Agata et al., 2014). Nevertheless, this study pointed out that using glacier inventories elaborated with different methodologies of data acquisition may lead to inaccuracies in the estimation of the total glacier area and, consequently, in the calculation of glacier surface variations (Salvatore et al., 2015).

Anyway, this study highlights the vulnerability of the Fumo Valley to climate change. The related effects, according to the future climatic scenarios, could be intensified in the next decades, with several implications for hydrological cycle, water resources, geomorphological hazards, landscape evolution, and ecosystem changes. Further studies are needed to assess the specific response of different abiotic and biotic systems to warming air temperature and cryosphere degradation in the study area (e.g., water runoff regime changes, paraglacial systems evolution, permafrost degradation, sediment connectivity changes, habitat loss, treeline shift).

## ACKNOWLEDGMENTS

The Author sincerely thanks Christian Casarotto for providing shapefile data related to the Italian Glacier Inventory and Roberto Seppi for providing shapefile data related to the Little Ice Age Trentino Glacier Inventory. Finally, the Author thanks the editor and the anonymous reviewer for their useful comments and improvements of the manuscript.

## Disclosure statement

The author declares that he has no known competing interests or personal relationships that could have appeared to influence the work reported in this paper.

## REFERENCES

- Ajassa R., Biancotti A., Brancucci G., Caputo C., Pugliese F. & Salvatore M.C. (1994) - Il Catasto dei Ghiacciai Italiani: primo confronto tra i dati 1958 e 1989. *Il Quaternario*, 7(1), 497-502.
- Auer I., Böhm R., Jurkovic A., Lipa W., Orlik A., Potzmann R., Schöner W., Ungersböck M., Matulla C., Briffa K., Jones P., Efthymiadis D., Brunetti M., Nanni T., Mauder M., Mercalli L., Mestre O., Moisselin J., Begert M., Müller-Westermeier G., Kveton V., Bochnicek O., Stastny P., Lapin M., Szalai S., Szentimrey T., Cegnar T., Dolinar M., Gajic-Capka M., Zaninovic K., Majstorovic Z. & Niepova E. (2007) - HISTALP— Historical instrumental climatological surface time series of the Greater Alpine Region. *Int. J. Climatol.*, 27, 17-46, <https://doi.org/10.1002/joc.1377>.
- Azzoni R.S., Fugazza D., Zerboni A., Senese A., D'Agata C., Maragno D., Carzaniga A., Cernuschi M. & Diolaiuti G.A. (2018) - Evaluating high-resolution remote sensing data for reconstructing the recent evolution of supra glacial debris a study in the Central Alps (Stelvio Park, Italy). *Progress in Physical Geography*, 42, 3-23, <https://doi.org/10.1177/0309133317749434>.
- Baffo F., Desiato F., Lena F., Suatoni B., Toreti A., Bider M., Cacciamani C. & Tinarelli G. (2005a) - Criteri di Calcolo degli indicatori meteorologici. Sistema nazionale di raccolta, elaborazione e diffusione di dati Climatologici di Interesse Ambientale, Agenzia per la Protezione dell'Ambiente e per i servizi Tecnici, 22 pp.
- Baffo F., Suatoni B. & Desiato F. (2005b) - Indicatori climatici: i controlli di validità e la ricerca dei valori errati. *Bollettino Geofisico*, a. XXVIII, n. 1-2, 31-41.
- Baroni C. & Carton A. (1990a) - Variazioni oloceniche della Vedretta della Lobbia (Gruppo dell'Adamello, Alpi Centrali). *Geogr. Fis. Dinam. Quat.*, 13, 105-119.
- Baroni C. & Carton A. (1990b) - Carta geomorfologica della V. Miller e della Conca dei Baitone (Gruppo dell'Adamello, Brescia). *Ann. Mus. Civ. Sc. Nat., Brescia*, 25, 5-25.
- Baroni C., Carton A. & Seppi R. (2004) - Distribution and Behaviour of Rock Glaciers in the Adamello-Presanella Massif (Italian Alps). *Permafrost and Periglac. Process.*, 15, 243-259, <https://doi.org/10.1002/ppp.497>.
- Baroni C., Martino S., Salvatore M.C., Mugnozza G.S. & Schilirò L. (2014) - Thermomechanical stress-strain numerical modelling of deglaciation since the Last Glacial Maximum in the Adamello Group (Rhaetian Alps, Italy). *Geomorphology*, 226, 278-299, <https://doi.org/10.1016/j.geomorph.2014.08.013>.
- Belloni S., Catasta G. & Smiraglia C. (1985) - Problematiche e indicazioni per un nuovo catasto dei ghiacciai italiani sulla base del confronto fra il Catasto Italiano 1959-1962 e il World Glacier Inventory. *Geogr. Fis. Dinam. Quat.*, 8, 166-181.

- Beniston M. (2003) - Climatic changes in mountain regions: A Review of Possible Impacts. *Climatic Change*, 59, 5-31, <https://doi.org/10.1023/A:1024458411589>.
- Bertoni E. & Casarotto C. (2015) - L'estensione dei ghiacciai trentini dalla fine della Piccola Età Glaciale a oggi. Rilevamento sul terreno, digitalizzazione GIS e analisi. Museo delle Scienze di Trento, Provincia Autonoma di Trento, 50 pp.
- Bianchi A., Callegari E. & Jobstraibizer P.G. (1970) - I tipi petrografici fondamentali del Plutone dell'Adamello (tonaliti, quarzodioriti, granodioriti e le loro varietà leucocrate). *Mem. Ist. Geol. Min. Univ. Padova*, 27, 148 pp.
- Bocchiola D. & Diolaiuti G. (2010) - Evidence of climate change within the Adamello glacier of Italy. *Theor. Appl. Climatol.*, 100, 351-369, <https://doi.org/10.1007/s00704-009-0186-x>.
- Brack P., Dal Piaz G.V., Baroni C., Carton A., Nardin M., Pellegrini G.B. & Pennacchioni G. (2008) - Note illustrative della Carta d'Italia alla scala 1:50.000, F. 58 Monte Adamello. Agenzia per la Protezione dell'Ambiente e per i Servizi Tecnici, Dipartimento di Difesa del Suolo Servizio Geologico d'Italia, Provincia Autonoma di Trento, 140 pp.
- Brahmbhatt R.M., Rathore B.P., Pattnaik S., Jani P., Bahuguna I., Shah R.D. & Rajawat A.S. (2015) - Peculiar characteristics of fragmentation of glaciers: A case study of Western Himalaya, India. *International Journal of Geosciences*, 6, 455-463, <https://doi.org/10.4236/ijg.2015.64035>.
- Brown L.E., Hannah D.M., Milner A.M., Soulsby C., Hodson A.J. & Brewer M.J. (2006) - Water source dynamics in a glacierized alpine river basin (Taillon-Gabitous, French Pyrénées). *Water Resour. Res.*, 42, W08404, <https://doi.org/10.1029/2005WR004268>.
- Brugnara Y., Brunetti M., Maugeri M., Nanni T. & Simolo C. (2012) - High-resolution analysis of daily precipitation trends in the central Alps over the last century. *Int. J. Climatol.*, 32, 1406-1422, <https://doi.org/10.1002/joc.2363>.
- Callegari E. (1983) - Note introduttive alla geologia del Massiccio dell'Adamello. In: Dal Piaz G.V. (Eds), *Il magmatismo tardo-alpino nelle Alpi, Escursione Adamello-Bregaglia*. Soc. Geol. It – Soc. It. Miner. Petr. Padova.
- Callegari E. (1985) - Geological and petrological aspects of the magmatic activity at Adamello (northern Italy). In: Dal Piaz G.V. (Eds), *Il magmatismo tardo alpino nelle Alpi*. *Mem. Soc. Geol. It.*, 26, 83-103.
- Callegari E. & Dal Piaz G.B. (1973) - Field relationships between the main igneous masses of the Adamello intrusive massif (Northern Italy). *Mem. Ist. Geol. Miner. Univ. Padova*, 29, 3-39.
- Callegari E. & Brack P. (2002) - Geological Map of the Tertiary Adamello Batholith (Northern Italy). Explanatory notes and legend. *Mem. Sci. Geol.*, 54, 19-49.
- Cannone N., Diolaiuti G., Guglielmin M. & Smiraglia C. (2008) - Accelerating climate impacts on alpine glacier forefield ecosystems in the European Alps. *Ecological Applications*, 18(3), 637-648, <https://doi.org/10.1890/07-1188.1>.
- Carton A. & Baroni C. (2017) - The Adamello-Presanella and Brenta Massifs Central Alps: Con-trasting High-Mountain Landscapes and Landforms. In: Soldati M. & Marchetti M. (Eds), *Land-scapes and Landforms of Italy, World Geomorphological Landscapes*, Springer, Cham, 101-112, [https://doi.org/10.1007/978-3-319-26194-2\\_8](https://doi.org/10.1007/978-3-319-26194-2_8).
- Ceppi P., Scherrer S.C., Fischer A.M. & Appenzeller C. (2012) - Revisiting Swiss temperature trends 1959–2008. *Int. J. Climatol.*, 32(2), 203-213, <https://doi.org/10.1002/joc.2260>.
- Chiarle M. & Mortara G. (2008) - Geomorphological impact of climate change on alpine glacial and periglacial areas. Examples of processes and description of research needs. *Interpraevent. Conference Proceedings*, 2, 111-122.
- Citterio M., Diolaiuti G., Smiraglia C., D'Agata C., Carnielli T., Stella G. & Siletto G.B. (2007) - The fluctuations of Italian Glaciers during the last century: a contribution to knowledge about alpine glacier change. *Geogr. Ann.*, 89(3), 167-184, <https://doi.org/10.1111/j.1468-0459.2007.00316.x>.
- Colombo N., Giaccone E., Paro L., Buffa G. & Fratianni S. (2016) - The recent transition from glacial to periglacial environment in a high altitude alpine basin (Sabbione Basin, North-Western Italian Alps). Preliminary outcomes from a multidisciplinary approach. *Geogr. Fis. Dinam. Quat.*, 39, 21-36, <https://doi.org/10.4461/GFDQ.2016.39.3>.
- Comitato Glaciologico Italiano – Consiglio Nazionale delle Ricerche (1959) - *Catasto dei Ghiacciai Italiani, Anno Geofisico Internazionale 1957-1958. Elenco generale e bibliografia dei ghiacciai italiani*. Comitato Glaciologico Italiano, Torino, 1, 172 pp.
- Comitato Glaciologico Italiano – Consiglio Nazionale delle Ricerche (1961a) - *Catasto dei Ghiacciai Italiani, Anno Geofisico Internazionale 1957-1958. Ghiacciai del Piemonte*. Comitato Glaciologico Italiano, Torino, 2, 324 pp.
- Comitato Glaciologico Italiano – Consiglio Nazionale delle Ricerche (1961b) - *Catasto dei Ghiacciai Italiani, Anno Geofisico Internazionale 1957-1958. Ghiacciai della Lombardia e dell'Ortles-Cevedale*. Comitato Glaciologico Italiano, Torino, 3, 389 pp.
- Comitato Glaciologico Italiano – Consiglio Nazionale delle Ricerche (1962) - *Catasto dei Ghiacciai Italiani, Anno Geofisico Internazionale 1957-1958. Ghiacciai delle Tre Venezie (escluso Ortles-Cevedale) e dell'Appennino*. Comitato Glaciologico Italiano, Torino, 4, 309 pp.
- D'Agata C., Bocchiola D., Maragno D., Smiraglia C. & Diolaiuti G. (2014) - Glacier shrinkage driven by climate change during half a century (1954-2007) in the Ortles-Cevedale group (Stelvio National Park, Lombardy, Italian Alps). *Theor. Appl. Climatol.*, 116, 169-190, <https://doi.org/10.1007/s00704-013-0938-5>.
- D'Agata C., Bocchiola D., Soncini A., Maragno D., Smiraglia C. & Diolaiuti G. (2018) - Recent area and volume loss of Alpine glaciers in the Adda River of Italy and their contribution to hydropower production. *Cold Reg. Sci. Technol.*, 148, 172-184, <https://doi.org/10.1016/j.coldregions.2017.12.010>.
- D'Agata C., Diolaiuti G., Maragno D., Smiraglia C. & Pelfini M. (2020) - Climate change effects on landscape and environment in glacierized Alpine areas: retreating glaciers and enlarging forelands in the Bernina Group (Italy) in the period 1954-2007. *Geology, Ecology and Landscapes*, 4(1), 71-86, <https://doi.org/10.1080/24749508.2019.1585658>.
- Deline P., Gruber S., Delaloye R., Fischer L., Geertsema M., Giardino M., Hasler A., Kirkbride M., Krautblatter M., Magnin F., McColl S., Ravel L. & Schoeneich P. (2015) - Ice Loss and Slope Stability in High-Mountain Regions. In: Shroder J.F., Haeberli W. & Whiteman C. (Eds), *Snow and Ice-related Hazards, Risks and Disasters. Hazards and Disasters Series*. Elsevier, 521-561, <https://doi.org/10.1016/B978-0-12-394849-6.00015-9>.
- Dempsey E.D., Holdsworth R.E., Imber J., Bistacchi A. & Di Toro G. (2014) - A geological explanation for intraplate earthquake clustering complexity: The zeolite-bearing fault/fracture networks in the Adamello Massif (Southern Italian Alps). *J. Struct. Geol.*, 66, 58-74, <https://doi.org/10.1016/j.jsg.2014.04.009>.
- Desiato F., Fioravanti G., Frascchetti P., Perconti W. & Piervitali E. (2015) - Valori climatici normali di temperatura e precipitazione in Italia. *Rapporto ISPRA, Serie Stato dell'Ambiente 55/2014*, 63 pp.
- Desiato F., Fioravanti G., Frascchetti P., Perconti W. & Toreti A. (2011) - Climate indicators for Italy: calculation and dissemination. *Adv. Sci. Res.*, 6, 147-150, <https://doi.org/10.5194/asr-6-147-2011>.

- Desiato F., Lena F. & Toreti A. (2007) - SCIA: a system for a better knowledge of the Italian climate. *Bollettino di Geofisica Teorica e Applicata*, 48(3), 351-358.
- Diolaiuti G., Azzoni R.S., D'Agata C., Maragno D., Fugazza D., Vagliasindi M., Mortara G., Perotti L., Bondesan A., Carton A., Pecci G., Dinale R., Trenti A., Casarotto C., Colucci R.R., Cagnati A., Crepez A. & Smiraglia C. (2019) - Present extent, features and regional distribution of Italian glaciers. *La Houille Blanche*, 105(5-6), 159-175, <https://doi.org/10.1051/lhb/2019035>.
- Diolaiuti G., Maragno D., D'Agata C., Smiraglia C. & Bocchiola D. (2011) - Glacier retreat and climate change: Documenting the last 50 years of Alpine glacier history from area and geometry changes of Dosedè Piazziglaciers (Lombardy Alps, Italy). *Progress in Physical Geography*, 35(2), 161-182, <https://doi.org/10.1177/0309133311399494>.
- Diolaiuti G. & Smiraglia C. (2010) - Changing glaciers in a changing climate: how vanishing geomorphosites have been driving deep changes in mountain landscapes and environments. *Géomorphologie: relief, processus, environnement*, 16(2), 131-152, <https://doi.org/10.4000/geomorphologie.7882>.
- Di Piazza A. & Eccel E. (2012) - Analisi di serie giornaliere di temperatura e precipitazione in Trentino nel periodo 1958-2010. Provincia Autonoma di Trento, Dipartimento Protezione Civile, Fondazione Edmund Mach, 92 pp.
- Dozier J. (1989) - Spectral signature of alpine snow cover from Landsat thematic mapper. *Remote Sens. Environ.*, 28, 9-22, [https://doi.org/10.1016/0034-4257\(89\)90101-6](https://doi.org/10.1016/0034-4257(89)90101-6).
- Drusch M., Del Bello U., Carlier S., Colin O., Fernandez V., Gascon F., Hoersch B., Isola C., Laberinti P., Martimort P., Meygret A., Spoto F., Sy O., Marchese F. & Bargellini P. (2012) - Sentinel-2: ESA's optical high-resolution mission for GMES operational services. *Remote Sens. Environ.*, 120, 25-36, <https://doi.org/10.1016/j.rse.2011.11.026>.
- Dyurgerov M.B. & Meier M.F. (2000) - Twentieth century climate change: evidence from small glaciers. *PNAS* 97(4), 1406-1411, <https://doi.org/10.1073/pnas.97.4.1406>.
- Eccel E., Cau P. & Ranzi R. (2012) - Data reconstruction and homogenization for reducing uncertainties in high-resolution climate analysis in Alpine regions. *Theor. Appl. Climatol.*, 110, 345-358, <https://doi.org/10.1007/s00704-012-0624-z>.
- EEA (2004) - Impacts of Europe's changing climate. An indicator-based assessment. EEA Report No. 2/2004. European Environment Agency, Copenhagen, Denmark.
- EEA (2009) - Regional climate change and adaptation: the Alps facing the challenge of changing water resources. EEA Report No. 8/2009. European Environment Agency, Copenhagen, Denmark.
- EEA (2017) - Climate change impacts and vulnerability in Europe 2016. An indicator-based report. EEA Report No. 1/2017. European Environment Agency, Copenhagen, Denmark.
- Fea M., Minora U., Pesaresi C. & Smiraglia C. (2013) - Remote sensing and interdisciplinary approach for studying glaciers. *Journal of Research and Didactics in Geography*, 2(2), 115-142, <https://doi.org/10.4458/2379-10>.
- Fioravanti G., Frascchetti P., Perconti W., Piervitali E. & Desiato F. (2016) - Controlli di qualità delle serie di temperatura e precipitazione. Rapporto ISPRA, Serie stato dell'Ambiente 66/2016, 34 pp.
- Gentili R., Baroni C., Panigada C., Rossini M., Tagliabue G., Armiraglio S., Citterio S., Carton A. & Salvatore M.C. (2020) - Glacier shrinkage and slope processes create habitat at high elevation and microrefugia across treeline for alpine plants during warm stages. *Catena*, 193, 104626, <https://doi.org/10.1016/j.catena.2020.104626>.
- Giaccone E., Colombo N., Acquavotta F., Paro L. & Fratianni S. (2015) - Climate variations in a high altitude Alpine basin and their effects on a glacial environment (Italian Western Alps). *Atmosfera*, 28(2), 117-128, [https://doi.org/10.1016/S0187-6236\(15\)30004-7](https://doi.org/10.1016/S0187-6236(15)30004-7).
- Gobiet A., Kotlarski S., Beniston M., Heinrich G., Rajczak J. & Stoffel M. (2014) - 21st century climate change in the European Alps – A review. *Sci. Total Environ.*, 493, 1138-1151, <https://doi.org/10.1016/j.scitotenv.2013.07.050>.
- Grossi G., Caronna P. & Ranzi R. (2013) - Hydrologic vulnerability to climate change of the Mandrone glacier (Adamello-Presanella group, Italian Alps). *Advances in Water Resources*, 55, 190-203, <https://doi.org/10.1016/j.advwatres.2012.11.014>.
- Guglielmin M., Bonasera M., Fubelli G., Tellini C. & Dramis F. (2022) - Permafrost-based geomorphology of the Mt. Foscagno – Mt. Forcellina ridge (Adda – Inn River basins, Central Italian Alps). *Journal of Maps*, 18(2), 441-447, <https://doi.org/10.1080/17445647.2022.2082331>.
- Guodong C. (1983) - Vertical and horizontal zonation of high-altitude permafrost. In: Péwé T.L. (Eds), 4th International Conference on Permafrost, Proceedings, Fairbanks, Alaska. National Academy Press, Washington D.C., 136-141.
- Haerberli W. & Beniston M. (1998) - Climate change and its impacts on glaciers and permafrost in the Alps. *Ambio*, 27, 258-265.
- Haerberli W., Bosch H., Scherler K., Østrem C. & Wallén C. (Eds). (1989) - World glacier inventory: Status 1988. Nairobi: IAHS(ICSI)/UNEP/ UNESCO/ World Glacier Monitoring Service.
- Haerberli W. & Gruber S. (2009) - Global warming and mountain permafrost. In: Margesin R. (Eds), *Permafrost Soils. Soil Biology V. 16*. Springer, Berlin, 205-2018, [https://doi.org/10.1007/978-3-540-69371-0\\_14](https://doi.org/10.1007/978-3-540-69371-0_14).
- Haerberli W., Hoelzle M., Paul F. & Zemp M. (2007) - Integrated monitoring of mountain glaciers as key indicators of global climate change: the European Alps. *Annals of Glaciology*, 46(1), 150-160, <https://doi.org/10.3189/172756407782871512>.
- Harris C., Arenson L.U., Christiansen H.H., Etzelmüller B., Frauenfelder R., Gruber S., Haerberli W., Hauck C., Hoelzle M., Humlum O., Isaksen K., Kääb A., Kern-Lütschag M.A., Lehning M., Matsuoka N., Murton J.B., Nötzli J., Phillips M., Ross N., Seppälä M., Springman S.M. & Mühl D.V. (2009) - Permafrost and climate in Europe: Monitoring and modelling thermal, geomorphological and geotechnical responses. *Earth-Science Reviews*, 92(3-4), 117-171, <https://doi.org/10.1016/j.earscirev.2008.12.002>.
- Hock R., Rasul G., Adler C., Cáceres B., Gruber Y., Hirabayashi Y., Jackson M., Kääb A., Kang S., Kutzov S., Milner A.I., Molau U., Morin S., Orlove B. & Steltzer H. (2019) - High Mountain Areas. In: Pörtner H.O., Roberts D.C., Masson-Delmotte V., Zhai P., Tignor M., Poloczanska E., Mintenbeck K., Alegria A., Nicolai M., Okem A., Petzold J., Rama B. & Weyer N.M. (Eds), *IPCC Special Report on the Ocean and Cryosphere in a Changing Climate*. Cambridge University Press, Cambridge, UK and New York, NY, USA, 131-202, <https://doi.org/10.1017/9781009157964.004>.
- IPCC (2021) - Climate Change 2021: The Physical Science Basis. Contribution of Working Group I to the Sixth Assessment Report of the Intergovernmental Panel on Climate Change [Masson-Delmotte V., Zhai V.P., Pirani A., Connors S.L., Péan C., Berger S., Caud N., Chen Y., Goldfarb L., Gomis M.I., Huang M., Leitzell K., Lonnoy E., Matthews J.B.R., Maycock T.K., Waterfield T., Yelekçi O., Yu R. & Zhou B. (Eds.)]. Cambridge University Press, Cambridge, United Kingdom and New York, NY, USA, 2391 pp., <https://doi.org/10.1017/9781009157896>.

- IUSS Working Group WRB (2015) - World Reference Base for Soil Resources 2014, update 2015. International soil classification system for naming soils and creating legends for soil maps. World Soil Resources Reports No. 106. FAO, Rome.
- Ivy-Ochs S., Kerschner H., Maisch M., Christl M., Kubik P.W. & Schlüchter C. (2009) - Latest Pleistocene and Holocene glacier variations in the European Alps. *Quaternary Science Reviews*, 28, 2137-2149, <https://doi.org/10.1016/j.quascirev.2009.03.009>.
- John B.E. & Blundy J.D. (1993) - Emplacement-related deformation of granitoid magmas, southern Adamello Massif, Italy. *Geol. Soc. Amer. Bull.*, 105, 1517-1541, [https://doi.org/10.1130/0016-7606\(1993\)105%3C1517:ERDOGM%3E2.3.CO;2](https://doi.org/10.1130/0016-7606(1993)105%3C1517:ERDOGM%3E2.3.CO;2).
- Jones D.B., Harrison S., Anderson K. & Whalley W.B. (2019) - Rock glaciers and mountain hydrology: A review. *Earth Science Reviews*, 193, 66-90, <https://doi.org/10.1016/j.earscirev.2019.04.001>.
- Kääb A., Winsvold S.H., Altena B., Nuth C., Nagler T. & Wuite J. (2016) - Glacier Remote Sensing Using Sentinel-2. Geometric Performance, and Application to Ice Velocity. *Remote Sens.*, 8(7), 598, <https://doi.org/10.3390/rs8070598>.
- Kottek M., Grieser J., Beck C., Rudolf B. & Rubel F. (2006) - World Map of the Köppen-Geiger climate classification updated. *Meteorologische Zeitschrift*, 15(3), 259-263, <https://doi.org/10.1127/0941-2948/2006/0130>.
- Maragno D., Diolaiuti G., D'Agata C., Mihalcea C., Bocchiola D., Bianchi Janetti E., Riccardi A. & Smiraglia C. (2009) - New evidence from Italy (Adamello Group, Lombardy) for analysing the ongoing decline of Alpine Glaciers. *Geogr. Fis. Dinam. Quat.*, 32, 31-39.
- Mercier D., Étienne S., Sellier D. & André M.F. (2009) - Paraglacial gullying of sediment-mantled slopes: a case study of Colletthøgda, Kongsfjorden area, West Spitsbergen (Svalbard). *Earth Surf. Process. Landforms*, 34, 1722-1789, <https://doi.org/10.1002/esp.1862>.
- Morino C., Conway S.J., Balme M.R., Helgason J.K., Sæmundsson P., Jordan C., Hillier J. & Argles T. (2021) - The impact of ground-ice thaw on landslide geomorphology and dynamics: two case studies in northern Iceland. *Landslides*, 18, 2785-2812, <https://doi.org/10.1007/s10346-021-01661-1>.
- Müller F., Caffisch T. & Müller G. (1977) - Instructions for Compilation and Assemblage of Data for a World Glacier Inventory. Temporary Technical Secretariat for World Glacier Inventory, International Commission on Snow and Ice, Zurich, 1-67.
- Nicholson L.I., McCarthy M., Pritchard H.D. & Willis I. (2018) - Supraglacial debris thickness variability: impact on ablation and relation to terrain properties, *The Cryosphere*, 12, 3719-3734, <https://doi.org/10.5194/tc-12-3719-2018>.
- Oerlemans J. (2005) - Extracting a climate signal from 169 glacier records. *Science*, 308, 675-677, <https://doi.org/10.1126/science.1107046>.
- Orombelli G. (2011) - Holocene mountain glacier fluctuations: a global overview. *Geogr. Fis. Dinam. Quat.*, 34, 17-24.
- Orombelli G., Ravazzi C. & Cita M.B. (2005) - Osservazioni sul significato dei termini LGM (UMG), Tardoglaciale e postglaciale in ambito globale, italiano ed alpino. *Il Quaternario*, 18(2), 147-155.
- Paul F., Barrand N.E., Baumann S., Berthier E., Bolch T., Casey K., Frey H., Joshi S.P., Konovalov V., Le Bris R., Mölg N., Nosenko G., Nuth C., Pope A., Racoviteanu A., Rastner P., Raup B., Scharrer K., Steffen S. & Winsvold S. (2013) - On the accuracy of glacier outlines derived from remote-sensing data. *Annals of Glaciology*, 54(63), 171-182, <https://doi.org/10.3189/2013AoG63A296>.
- Paul F., Huggel C. & Kääb A. (2004a) - Combining satellite multispectral image data and a digital elevation model for mapping debris-covered glaciers. *Remote sensing of Environment*, 89, 510-518, <http://dx.doi.org/10.1016/j.rse.2003.11.007>.
- Paul F., Kääb A. & Haeberli W. (2007) - Recent glacier changes in the Alps observed by satellite: Consequences for future monitoring strategies. *Global and Planetary Change*, 56, 111-122, <https://doi.org/10.1016/j.gloplacha.2006.07.007>.
- Paul F., Kääb A., Maisch M., Kellenberger T. & Haeberli W. (2004b) - Rapid disintegration of Alpine glaciers observed with satellite data. *Geophysical Research Letters*, 31, L21402, <https://doi.org/10.1029/2004GL020816>.
- Paul F., Rastner P., Azzoni R.S., Diolaiuti G., Fugazza D., Le Bris R., Nemec J., Rapatel A., Ramusovic M., Schwaizer G. & Smiraglia C. (2020) - Glacier shrinkage in the Alps continues unabated as revealed by a new glacier inventory from Sentinel-2. *Earth Syst. Sci. Data*, 12, 1805-1821, <https://doi.org/10.5194/essd-12-1805-2020>.
- Paul F., Winsvold S.H., Kääb A., Nagler T. & Schwaizer G. (2016) - Glacier Remote Sensing Using Sentinel-2. Part II: Mapping Glacier Extents and Surface Facies, and Comparison to Landsat 8. *Remote Sens.*, 8(7), 575, <https://doi.org/10.3390/rs8070575>.
- Ravazzani G., Dalla Valle F., Mendlik T., Galeati G., Gobiet A. & Mancini M. (2015) - Assessing Climate Impacts on Hydropower Production of Toce Alpine Basin. In: Lollino G., Manconi A., Clague J., Shan W. & Chiarle M. (2015). *Engineering Geology for Society and Territory - Volume 1. Climate Change and Engineering Geology*, Springer, 9-12, [https://doi.org/10.1007/978-3-319-09300-0\\_2](https://doi.org/10.1007/978-3-319-09300-0_2).
- Rubel F., Brugger K., Haslinger K. & Auer I. (2017) - The climate of the European Alps: shift of very high resolution Köppen-Geiger climate zones 1800-2100. *Meteorologische Zeitschrift*, 26(2), 115-125, <https://doi.org/10.1127/metz/2016/0816>.
- Salvatore M.C., Zanoner T., Baroni C., Carton A., Banchieri F.A., Viani C., Giardino M. & Perotti L. (2015) - The state of Italian Glaciers: a snapshot of the 2006-2007 hydrological period. *Geogr. Fis. Dinam. Quat.*, 38, 175-198, <https://doi.org/10.4461/GFDQ.2015.38.16>.
- Sartori G., Mancabelli A., Wolf U. & Corradini F. (2005) - *Atlante dei suoli del Parco Naturale Adamello-Brenta. Suoli e paesaggi. Museo Tridentino di Scienze Naturali. Monografie II*, 239 pp.
- Schoeneich P., Dall'Amico M., Deline P., Zischg A. (2011) - Hazards related to permafrost and to permafrost degradation. *PermaNET project, State of the Art Report, Action 6.2*.
- Seppi R., Carton A., Zumiani M., Dall'Amico M., Zampedri G. & Rigon R. (2012) - Inventory, distribution and topographic features of rock glaciers in the Southern Region of the Eastern Italian Alps (Trentino). *Geogr. Fis. Dinam. Quat.*, 35, 185-197, <http://dx.doi.org/10.4461/GFDQ.2012.35.17>.
- Seppi R., Carturan L., Carton A., Zanoner T., Zumiani M., Cazorzi F., Bertone A., Baroni C. Salvatore M.C. (2019) - Decoupled kinematics of two neighbouring permafrost creeping landforms in the Eastern Italian Alps. *Earth Surf. Process. Landforms*, 44, 2703-2719, <https://doi.org/10.1002/esp.4698>.
- Serandrei-Barbero R. & Zanon G. (1993) - The Italian Alps. In: Williams R.S. & Ferrigno J.G. (Eds), *Satellite image atlas of glaciers of the world - Europe*, USGS Professional Paper 1386-E. Washington D.C., USGS.
- Slaymaker O. (2011) - Criteria to distinguish between periglacial, proglacial and paraglacial environments. *Quaestiones Geographicae*, 30(1), 85-94, <https://doi.org/10.2478/v10117-011-0008-y>.
- Smiraglia C., Azzoni R.S., D'Agata C., Maragno D., Fugazza D. & Diolaiuti G. (2015) - The evolution of the Italian glaciers from the previous database to the New Italian Inventory. Preliminary considerations and results. *Geogr. Fis. Dinam. Quat.*, 38, 79-87, <http://dx.doi.org/10.4461/GFDQ.2015.38.08>.

- Smiraglia C. & Diolaiuti G. (Eds.) (2015) - Il Nuovo Catasto dei Ghiacciai Italiani. Ev-K2-CNR Ed., Bergamo, 400 pp.
- Sommer C., Malz P., Seehaus T.C., Lippl S., Zemp M. & Braun M.H. (2020) - Rapid glacier retreat and downwasting throughout the European Alps in the early 21st century. *Nature Communications*, 11, 3209, <https://doi.org/10.1038/s41467-020-16818-0>.
- Viviroli D. & Weingartner R. (2004) - The hydrological significance of mountains: from regional to global scale. *Hydrology and Earth Sciences*, 8(6), 1016-1029, <https://doi.org/10.5194/hess-8-1017-2004>.
- World Glacier Monitoring Service & National Snow and Ice Data Center (1999) - World Glacier Inventory, Version 1 [Data Set]. Boulder, Colorado USA. National Snow and Ice Data Center, <https://doi.org/10.7265/N5/NSIDC-WGI-2012-02>.
- World Meteorological Organization (2015) - Technical Regulations, Basic documents no. 2, Vol. I. General Meteorological Standards and Recommended Practices. 2015 Edition, Updated in 2017. WMO-No. 49, Geneva.
- World Meteorological Organization (2017) - WMO Guidelines on the Calculation of Climate Normals. 2017 Edition. WMO-No. 1203, Geneva.
- Zanoner T., Carton A., Seppi R., Carturan L., Baroni C., Salvatore M.C. & Zumiani M. (2017) - Little Ice Age mapping as a tool for identifying hazard in the paraglacial environment: the case study of Trentino (Eastern Italian Alps). *Geomorphology*, 295, 551-562, <https://doi.org/10.1016/j.geomorph.2017.08.014>.
- Zanon G. (1985) - L'attuale tendenza evolutiva dei Ghiacciai delle Alpi italiane. *Geogr. Fis. Dinam. Quat.*, 8, 89-96.
- Zemp M., Haeberli W., Hoelzle M. & Paul F. (2006) - Alpine Glaciers to disappear within decades? *Geophysical Research Letters*, 33, L13504, <https://doi.org/10.1029/2006GL026319>.